

STRUCTURAL DYNAMICS EXPERIMENTS ON ESA SPACE LAUNCHERS

Giuliano Coppotelli, Daniele Antonini, Ludovica Onofri

DIPARTIMENTO DI INGEGNERIA
MECCANICA E AEROSPAZIALE



SAPIENZA
UNIVERSITÀ DI ROMA



IOMAC2027 OMA LECTURE SERIES

April 09th, 2026

Agenda

1. Motivations
2. Theoretical Background on OMA approaches
3. OMA on ARIANE Launch Vehicle
4. OMA on VEGA P80 Motor
5. OMA on REXUS36 Sounding Rocket
6. Concluding Remarks

➤ Topics at glance

- ❑ The development of OMA methods allows estimating the modal parameters of a structural system by using **vibration responses only**
- ❑ The OMA methodologies are of great importance from the industrial point of view **permitting to evaluate the behavior** of a structure **under its operative conditions**
- ❑ The **dynamic identification of a Launch Vehicle** structure under its actual operative conditions is of great importance for **launcher industry**
 - Updating numerical models of the structure and for improving the design
 - High operative costs for the experimental acquisition also in ground testing
 - Reducing the time-to-market in the developing phase

- Main advantages from Output-Only analysis
 - ❑ Operational Modal Analysis for time-varying systems
 - ❑ Root locus estimate and Time-Tracking of the modal parameters
 - ❑ Accuracy evaluation of the numerical prediction and model updating
 - ❑ Identification of (possible) harmonic interactions due to combustion dynamics
 - ❑ Validation of the sensor placement methodologies using time-dependent mode shapes
 - ❑ Evaluation of the effects of dynamic range of measurements in the modal parameter estimate and tracking
 - ❑ Estimate rocket performances by integrating numerical simulations
- Validation of the developed methodology
 - ❑ Numerical analyses
 - ❑ Firing test
 - ❑ Flight tests

Agenda

1. Motivations
2. Theoretical Background on OMA approaches
3. OMA on ARIANE Launch Vehicle
4. OMA on VEGA P80 Motor
5. OMA on REXUS36 Sounding Rocket
6. Concluding Remarks

Natural Input Modal Analysis



IOMAC2027 OMA

DYNAMICS EXPERIMENTS ON ESA SPACECRAFT LAUNCHERS

Natural Input Modal Analysis: N.I.M.A.

© Department of Mechanical and Aerospace Engineering
University of Rome "La Sapienza"

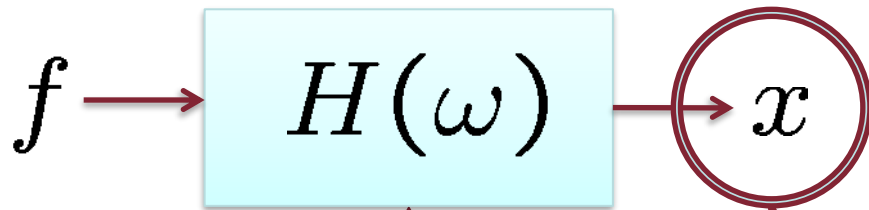
Hilbert Transform Method
(HTM)

Frequency Domain Decomposition
(FDD)

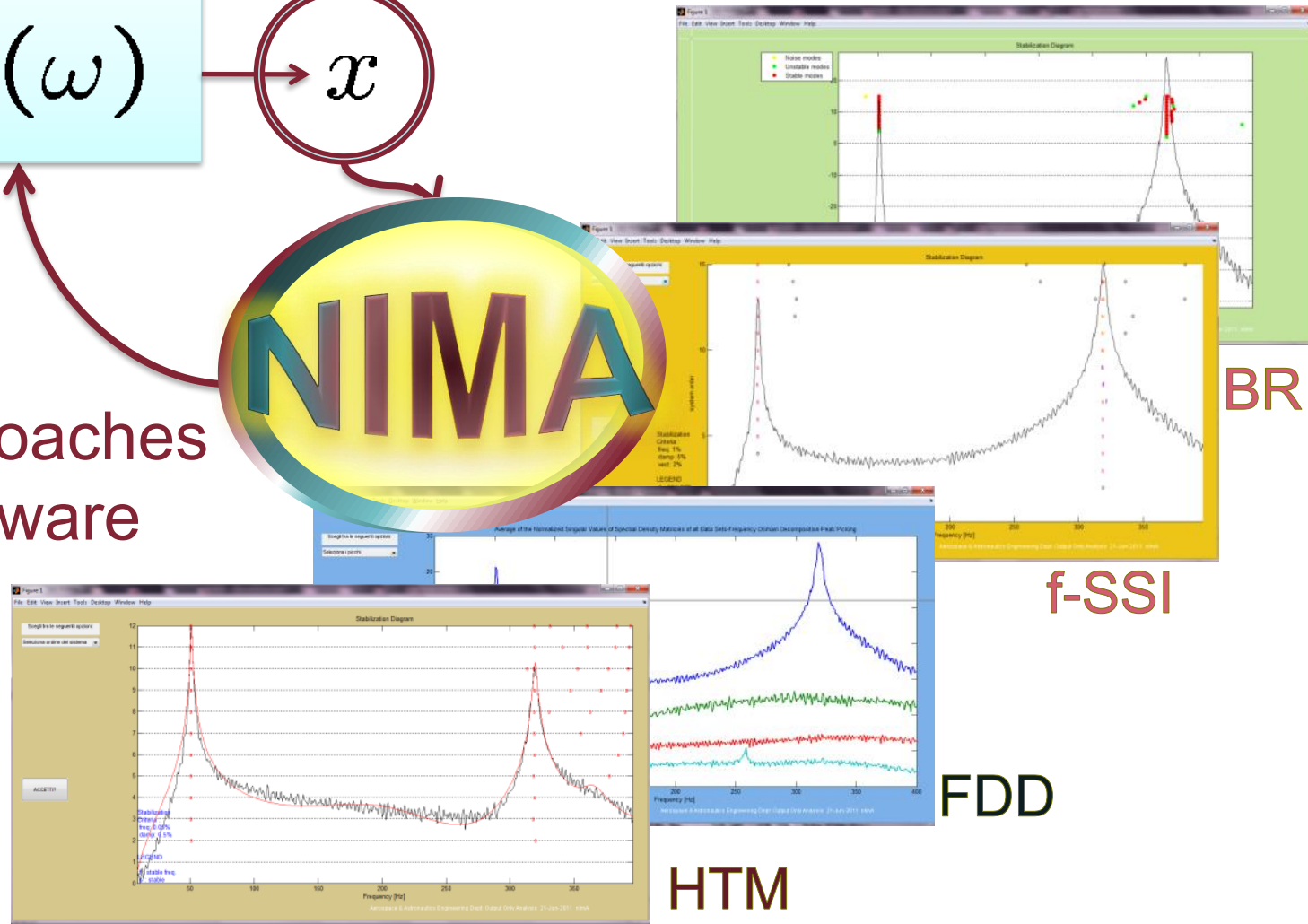
Stochastic Modal
Appropriation
(SMA)
Ready to be implemented



Stochastic Subspace Identification (SSI)
Time & Frequency domain



Multiple Approaches
Single Software





and also

Natural Frequencies

Damping Ratios

Normal Modes

Mode scaling



Harmonic removal



Accuracy of the estimates: some remarks

- ❑ From the mathematical point of view the **dynamics** of a system is **defined by its poles** (state matrix eigenvalues) λ_n
- ❑ The **OMA techniques provide** estimates of the system dynamics by identifying the **natural frequencies** f_n and **damping ratios** ζ_n
- ❑ Once natural frequencies and damping ratios are estimated the poles of the system are identified

$$\lambda_n = \lambda_{R_n} + j\lambda_{I_n}$$

$$\zeta_n := -\frac{\lambda_{R_n}}{\lambda_{I_n}}$$

$$\lambda_{n_I} := \omega_n = 2\pi f_n$$

- ❑ If the poles (in general complex) are written in the complex plane in module and phase

$$|\lambda_n| = \omega_n \sqrt{1 + \zeta_n^2} \cong \omega_n$$

$$\angle \lambda_n = \frac{\pi}{2} + \arctan(\zeta_n) \cong \frac{\pi}{2} + \zeta_n$$

- ❑ By introducing the uncertainties associated to the estimate quantities $\Delta\zeta_n$ and Δf_n

$$\Delta|\lambda_n| \cong 2\pi\Delta f_n = O(1)$$

$$\Delta\angle\lambda_n \cong \Delta\zeta_n = O(10^{-2})$$

- ❑ The **system poles** are practically identified within the **uncertainties associated to the natural frequencies**
- ❑ **The system dynamics is identified by the uncertainties associated to its natural frequencies**

A criterion of applicability for time-varying systems

- ❑ The **OMA hypotheses** require a **linear time-independent system excited by a white noise**
- ❑ If the system is characterized by **time-dependent dynamic** properties, the analysis can be carried out by splitting the whole observation time **into sub-intervals** where the **system dynamical features** can be considered as **time-independent**
- ❑ The **system dynamics is identified by the natural frequencies uncertainties**: the presented criterion is based on the frequencies

- The frequency is identified within an error associated to the frequency resolution Δf_n
- The frequency can be represented by a reference value plus its time-variation in the
 - observation-window

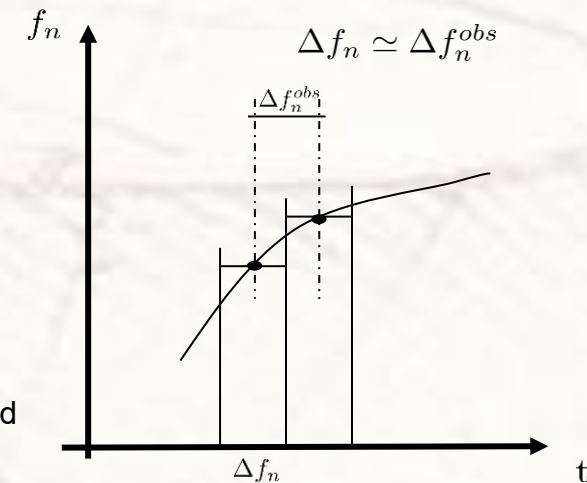
$$f_n = \check{f}_n + \Delta_{obs} f_n$$

- To apply the OMA methods and thus consider the system as time-invariant, it must hold

$$\Delta_{obs} f_n \leq \Delta f_n = 1/\Delta t$$

$$\text{with } \Delta_{obs} f_n = \dot{f}_n \Delta t \quad \dot{f}_n = \max_I [\dot{f}(t)] \quad t \in [t_I, t_I + \Delta t]$$

- Thus, the applicability criterion, linking frequency resolution and time-variation, is obtained: $\Delta t \leq \sqrt{\frac{1}{\dot{f}_n}}$



Agenda

1. Motivations
2. Theoretical Background on OMA approaches
3. OMA on ARIANE Launch Vehicle
4. OMA on VEGA P80 Motor
5. OMA on REXUS36 Sounding Rocket
6. Concluding Remarks



3. OMA on ARIANE Launch Vehicle

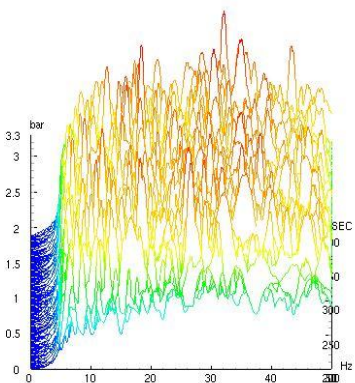
1/16



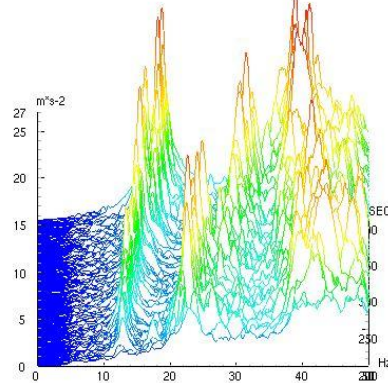
Signal data characterization

- Flight phase where the system is excited by a supposed white noise
- The responses are recorded in correspondence of 4 locations left intentionally unknown.
- Three different experimental cases (corresponding to the same flight phase) have been recorded and analyzed: Flight#1, Flight#2, Flight#3
- Target modes around 10/20Hz and 30/40Hz
- The analysis is performed in the time-window [200s-500s]
- For the given signal data 30 intervals I_i , $i=1, \dots, 30$, of 10 seconds are considered (compromise between frequency resolution and supposed frequency time-variation)
- Frequency resolution 0.1Hz and Nyquist frequency of 227.27Hz

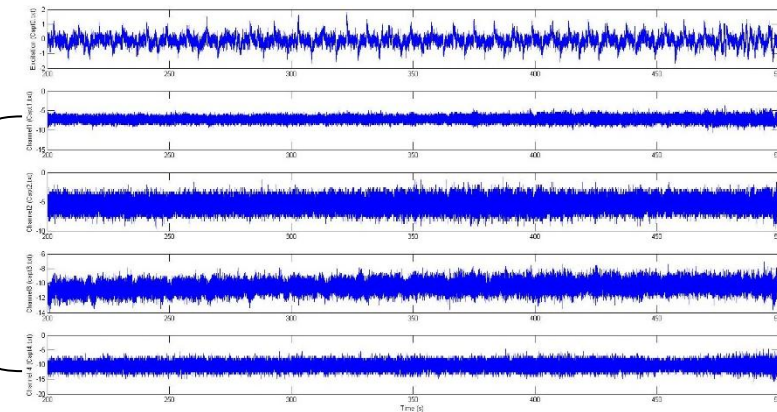
Excitation Spectra



Response Spectra



Excitation



Channels

3. OMA on ARIANE Launch Vehicle

2/16

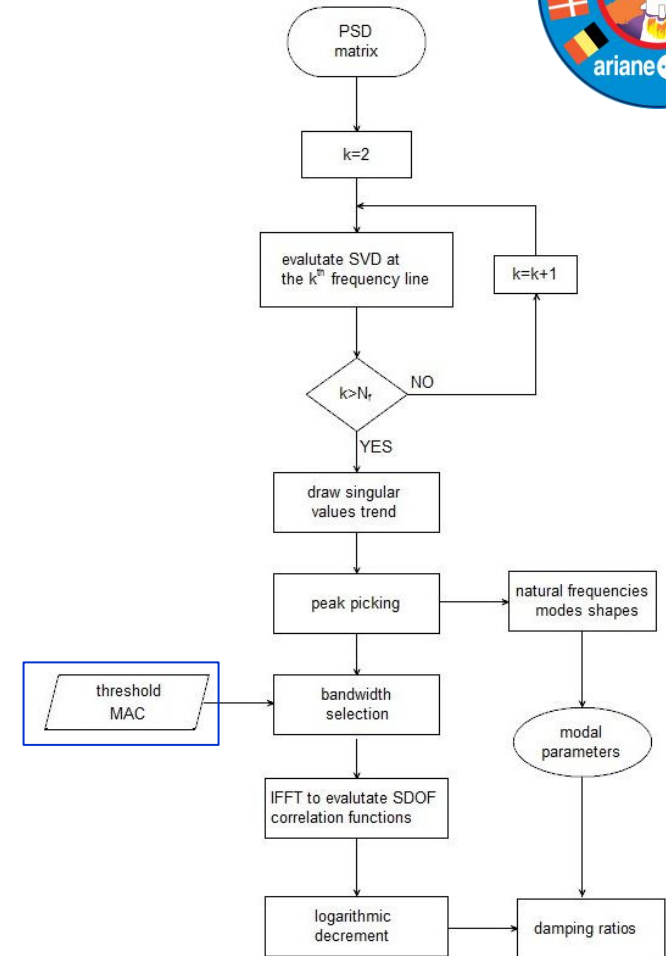


FDD numerical procedure

- ❑ Computation of the PDS matrix $\forall \omega_k$
- ❑ Evaluation of the SVD of the PSD matrix
- ❑ The natural frequencies f_n obtained from the Singular Values trend
- ❑ The damping ratios ζ_n are obtained from the logarithmic decrement

Analysis parameters in the estimation procedure:

- Threshold MAC=0.9



FDD flow diagram of NIMA code

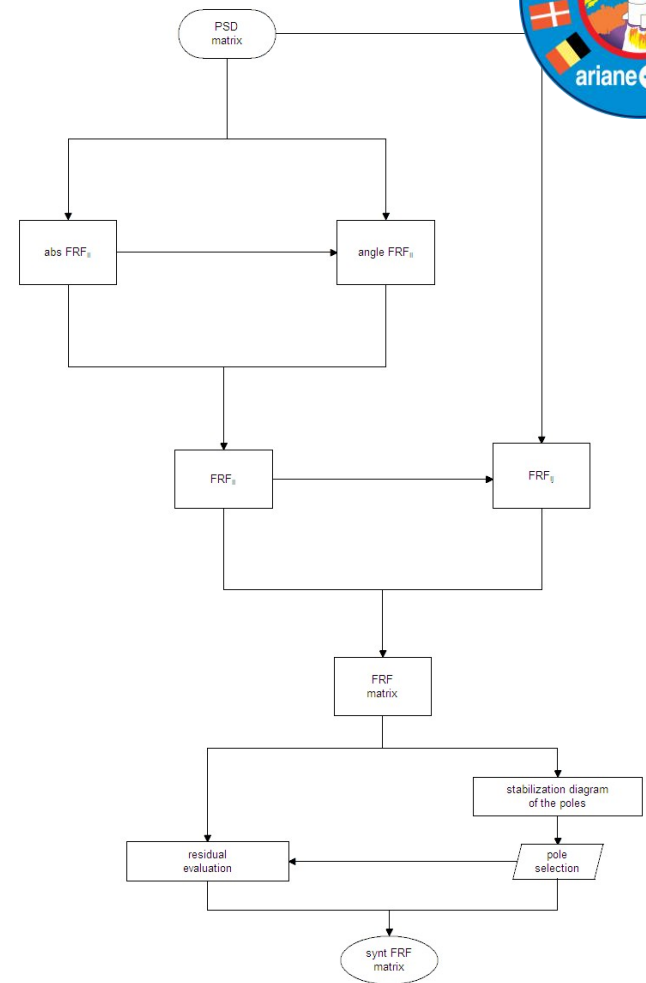
3. OMA on ARIANE Launch Vehicle

3/16



HTM numerical procedure

- ❑ Computation of the PDS matrix
- ❑ Evaluation of the FRF via the Hilbert Transform of the PSD matrix
- ❑ The system poles (f_n and ζ_n) are identified via stabilization diagram

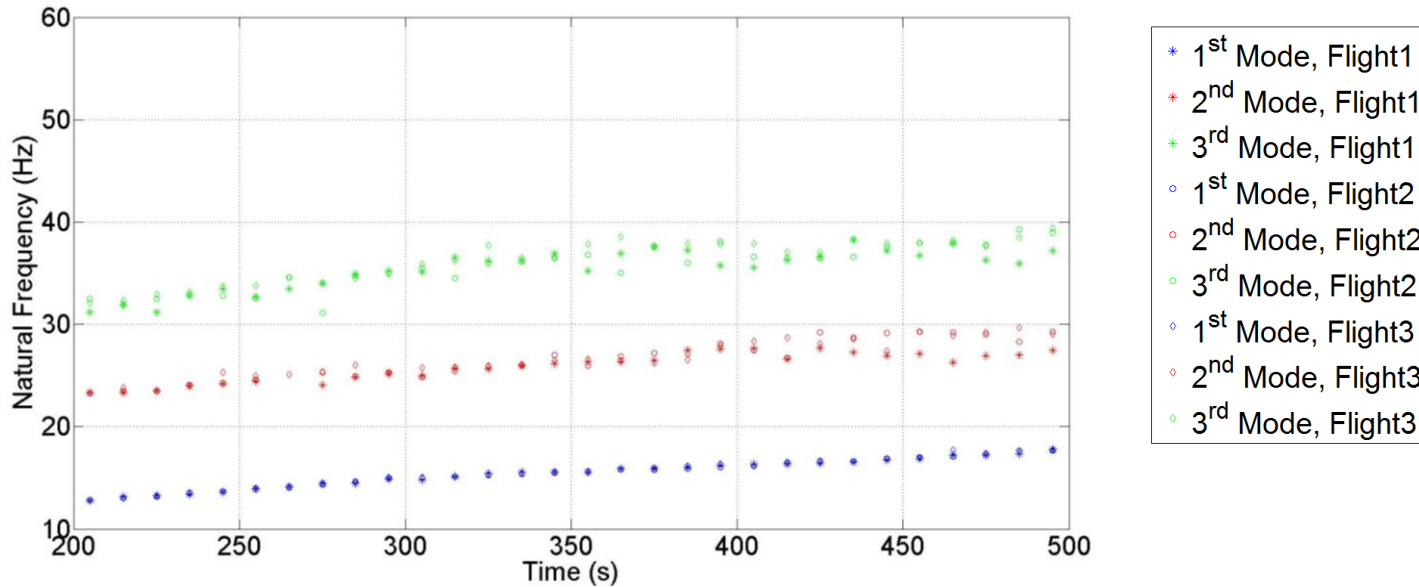


3. OMA on ARIANE Launch Vehicle

4/16



Identified natural frequencies using FDD



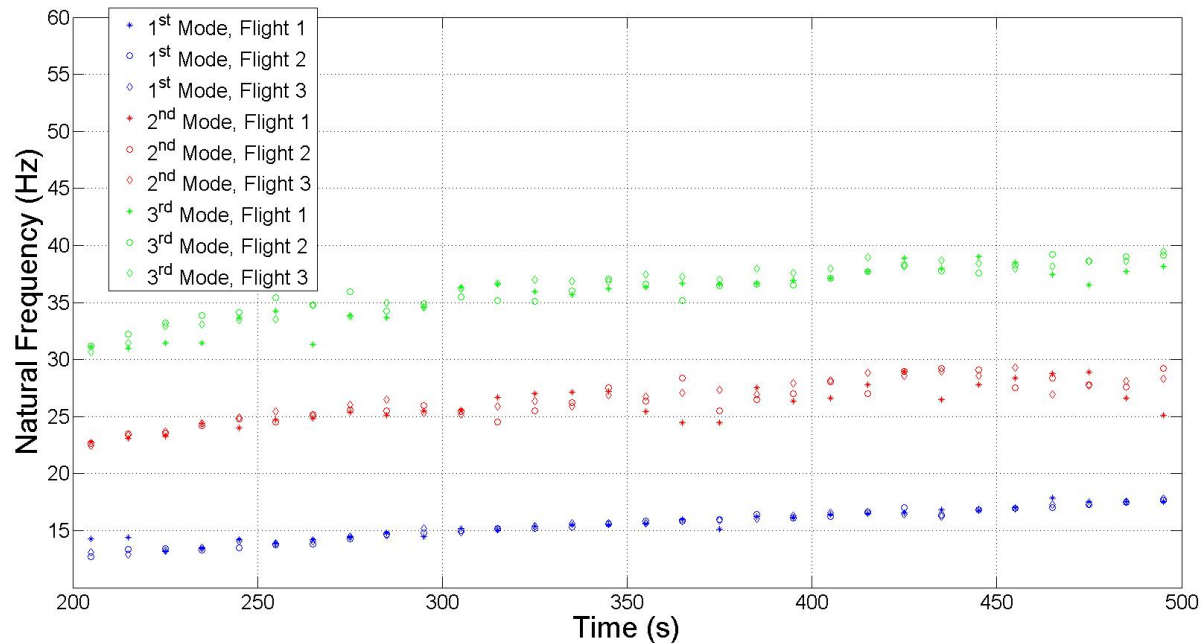
- For all the flights the natural frequencies have been identified**
- For all the flights the time-varying trend of natural frequencies have been tracked**
- The identified natural frequencies in different flights (for the same mode and same time) differ for a max of about 5 Hz
- The difference between the estimates among different flight increases with the mode order

3. OMA on ARIANE Launch Vehicle

5/16



Identified natural frequencies using HTM



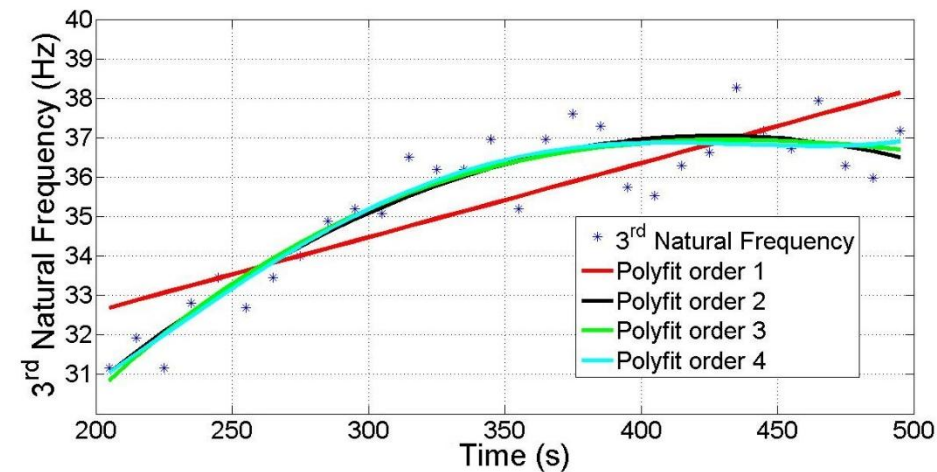
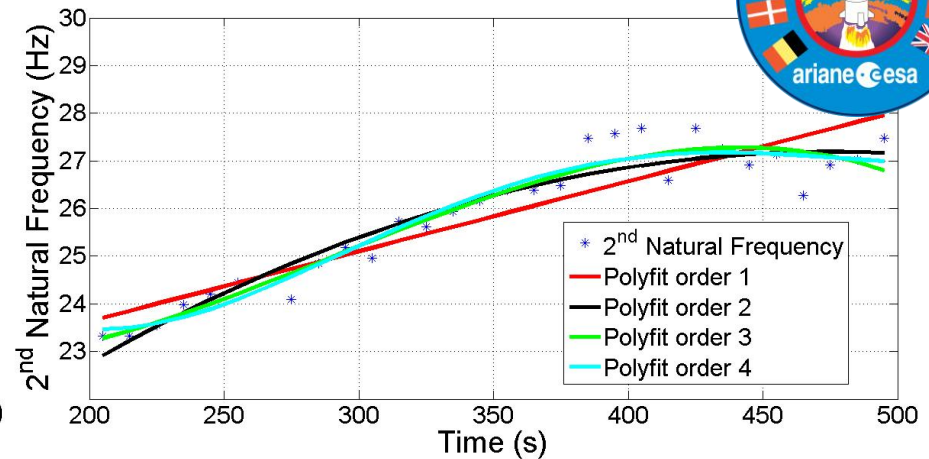
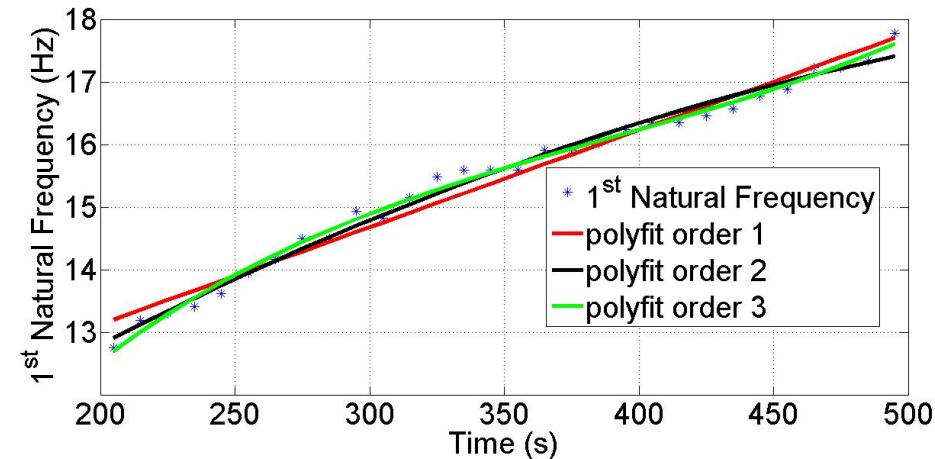
- For all the flights the natural frequencies have been identified
- For all the flights the time-varying trend of natural frequencies have been tracked
- The identified frequencies in different flights (for the same mode and same time) differ for a max of about 5 Hz
- The difference between the estimates among different flight increase with the mode order

3. OMA on ARIANE Launch Vehicle

6/16



Tracking of the natural frequencies using FDD, Flight #1



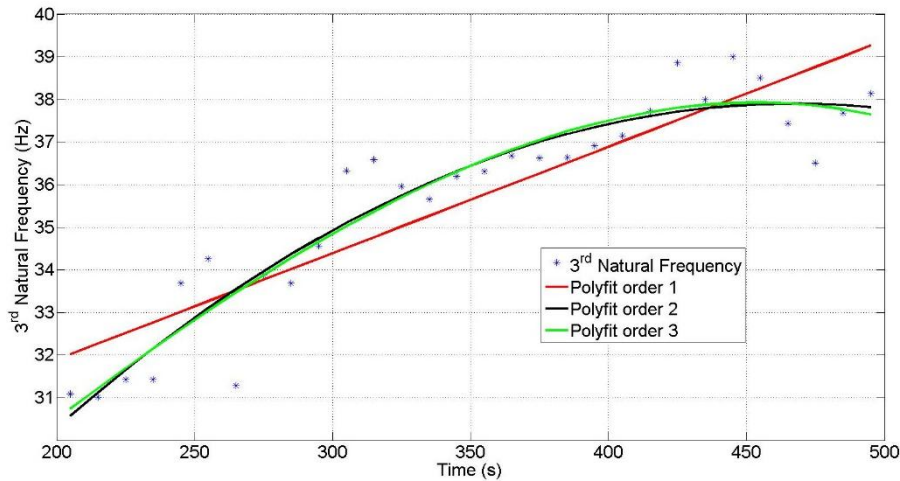
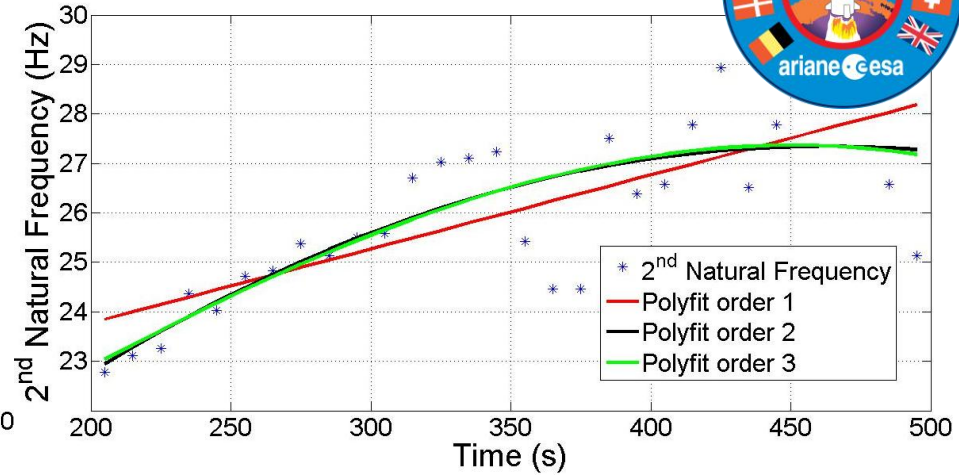
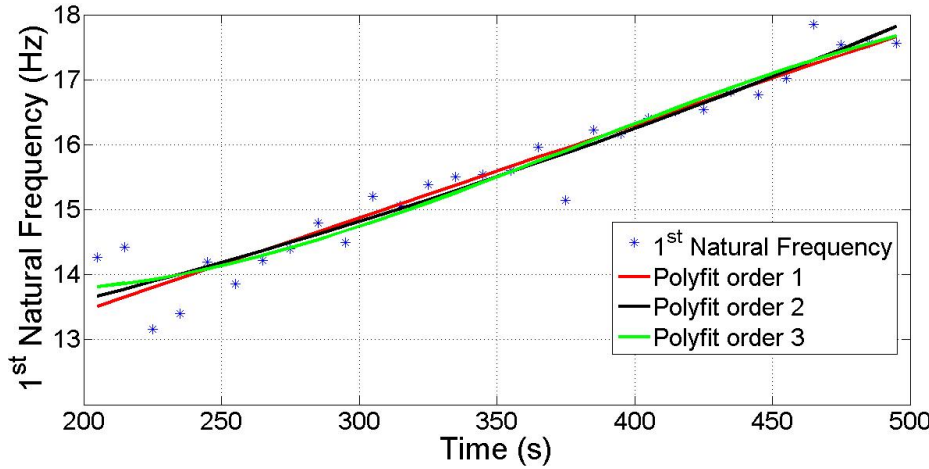
- Similar trends have been obtained for Flight#2 and Flight#3
- The target frequencies have globally been identified and time-tracked
- The 2nd natural frequency has not been identified in the interval [260s, 270s] due to too high uncertainties in Flight#1 and Flight#2

3. OMA on ARIANE Launch Vehicle

7/16



Tracking of the natural frequencies using HTM, Flight #1



Similar trends have been obtained for Flight#2 and Flight3

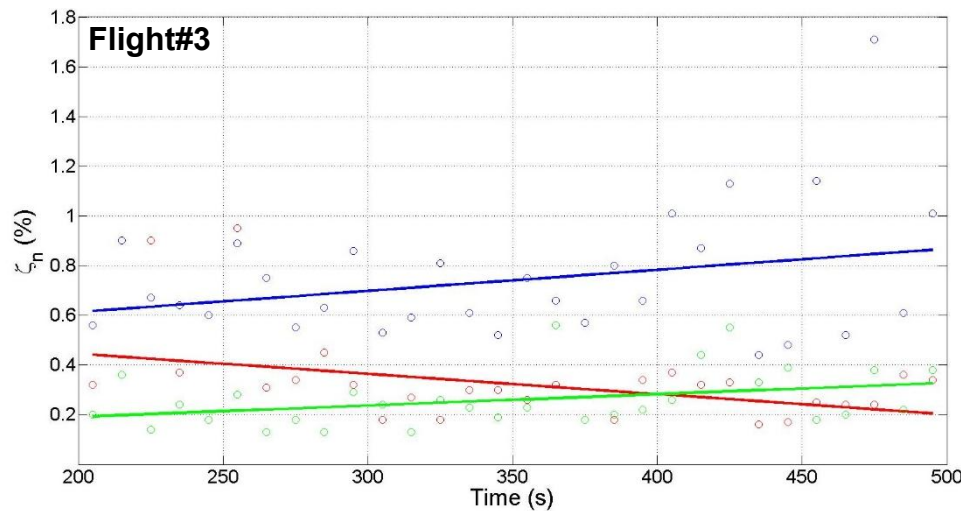
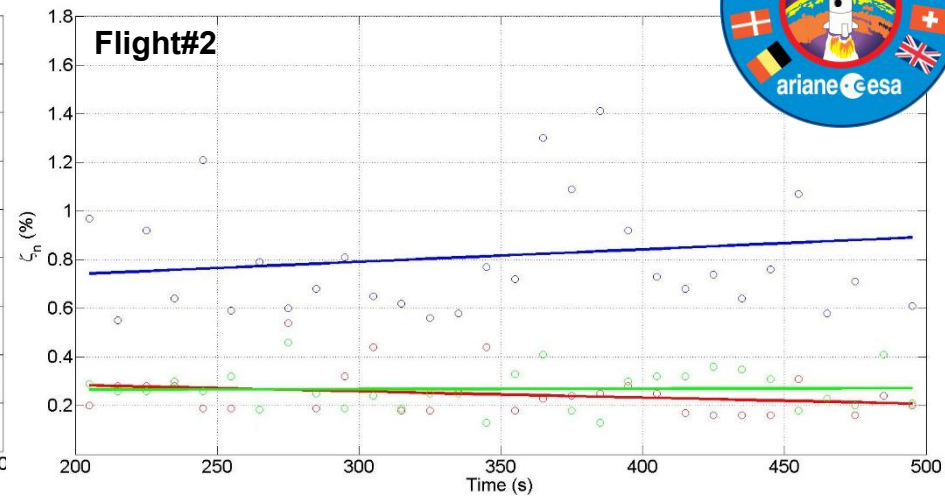
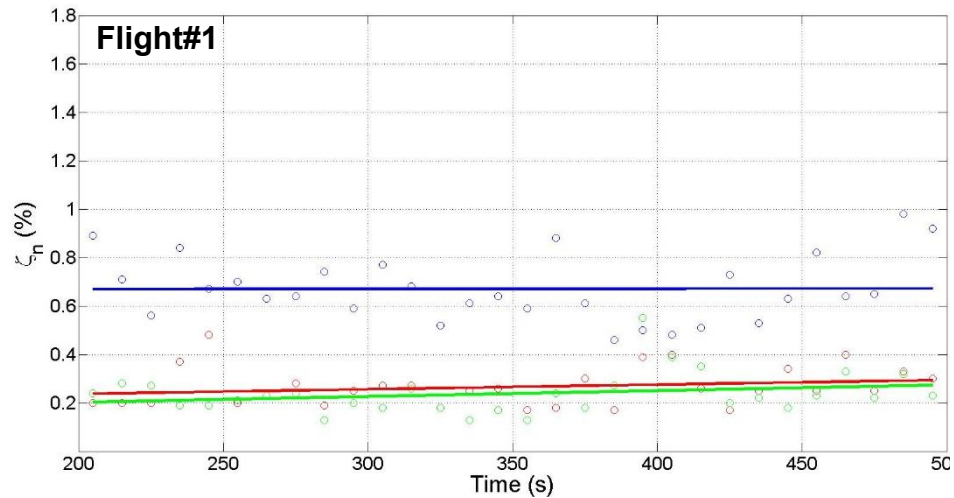
The target frequencies have been identified and time-tracked

3. OMA on ARIANE Launch Vehicle

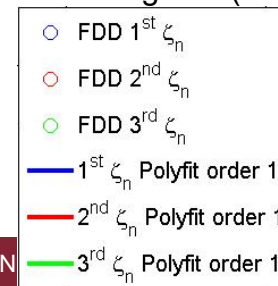
8/16



Tracking of the damping ratios using FDD



- The damping ratios have been globally identified and time-tracked
- Strongly dependent on the considered flight by considering the single value
- Similar intervals of variation
- In the interval [260s, 270s] the damping ratio are not identified for Flight#1 and Flight#2 (because are not identified the frequencies)

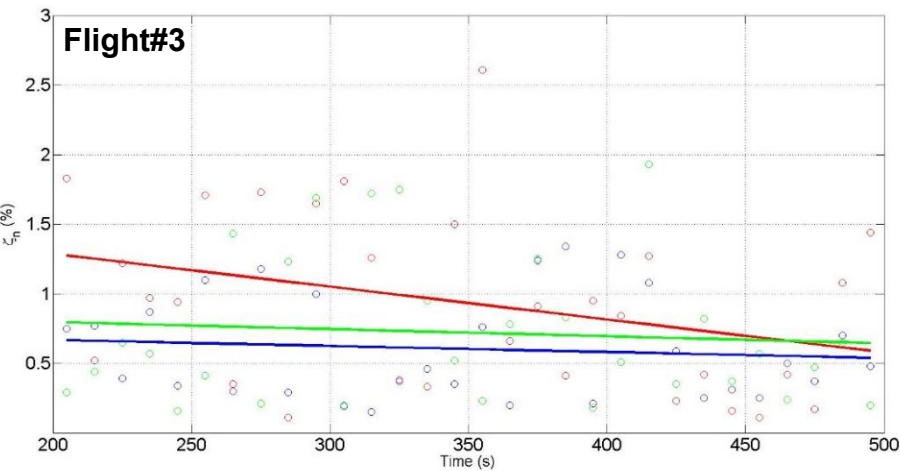
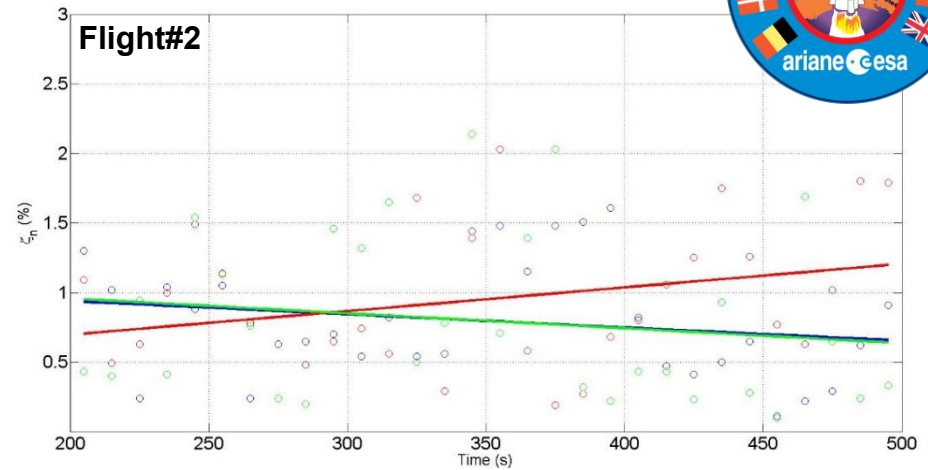
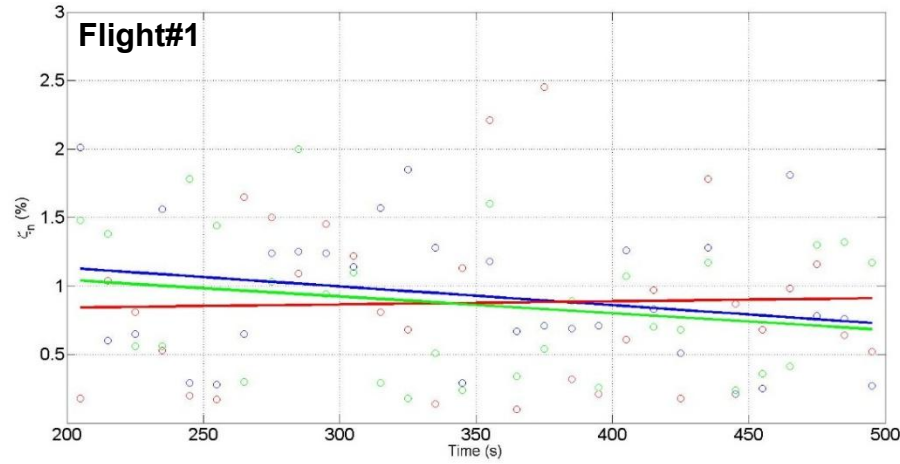


3. OMA on ARIANE Launch Vehicle

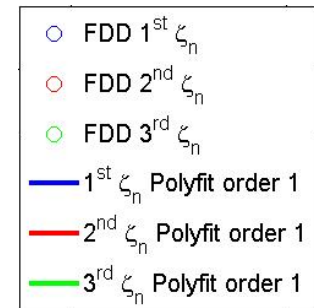
9/16



Tracking of the damping ratios using HTM



- ❑ The damping ratios have been identified and time-tracked
- ❑ Strongly dependent on the considered flight by considering the single value
- ❑ Similar intervals of variation

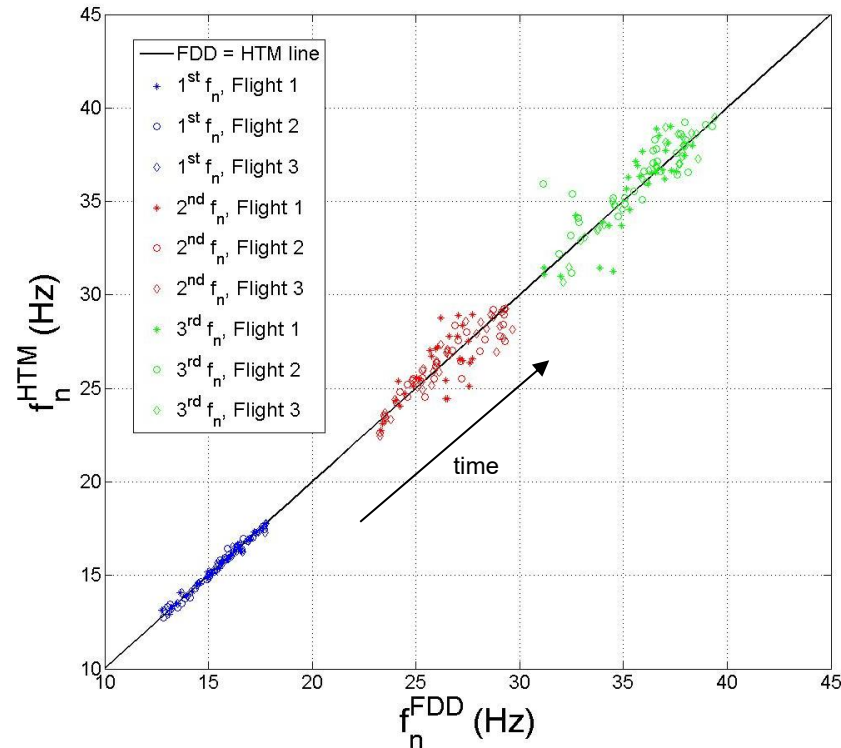


3. OMA on ARIANE Launch Vehicle

10/16



HTM vs FDD natural frequencies comparison



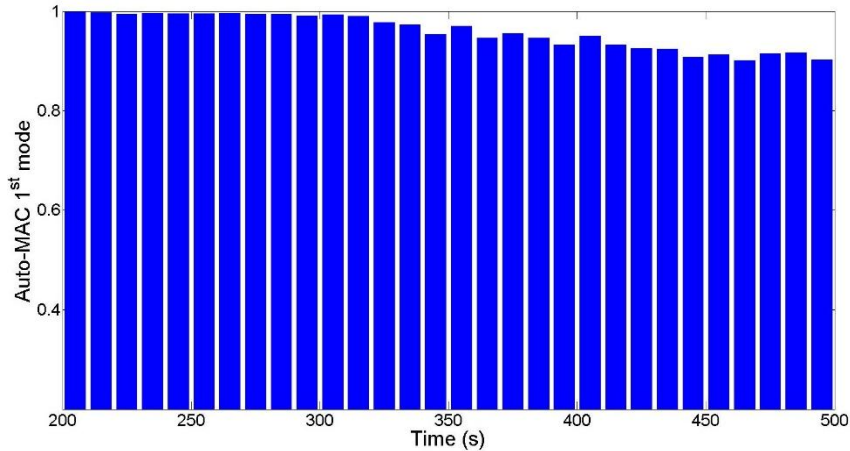
- ❑ The first frequency is the best identified
- ❑ The higher the order of the corresponding modes the higher the differences within the estimates among different flights
- ❑ The largest difference among the identified frequency with FDD and HTM is around 5Hz

3. OMA on ARIANE Launch Vehicle

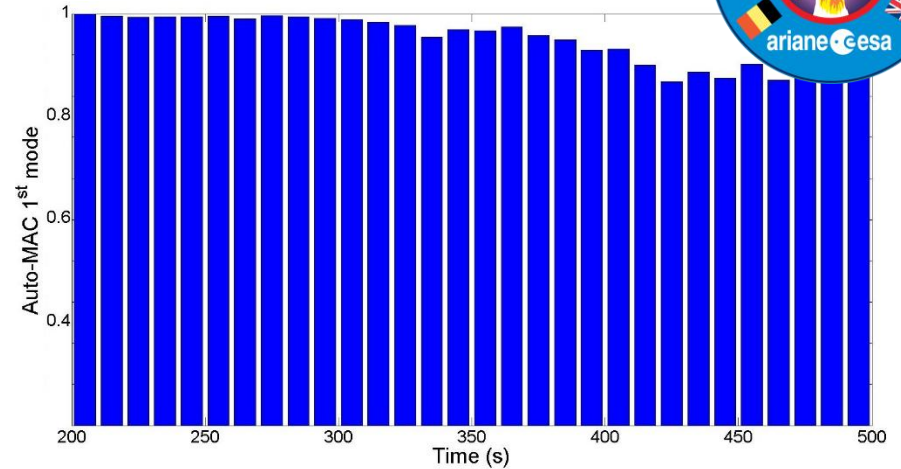


Tracking of the 1st mode shape using FDD

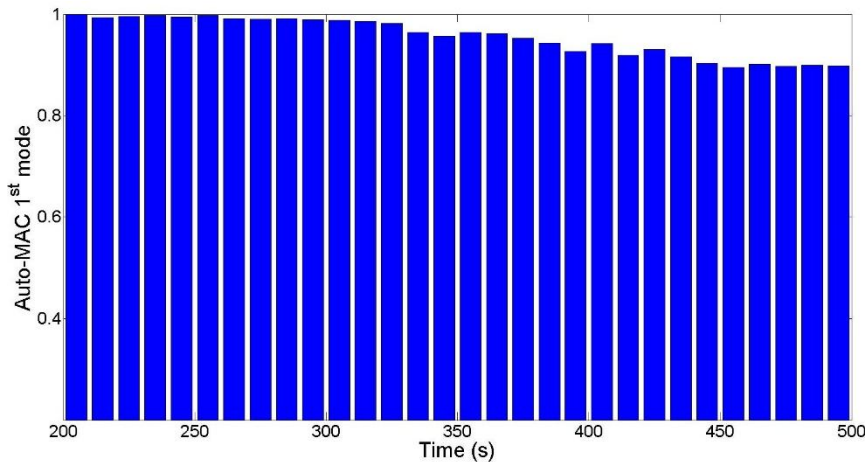
Flight#1



Flight#2



Flight#3



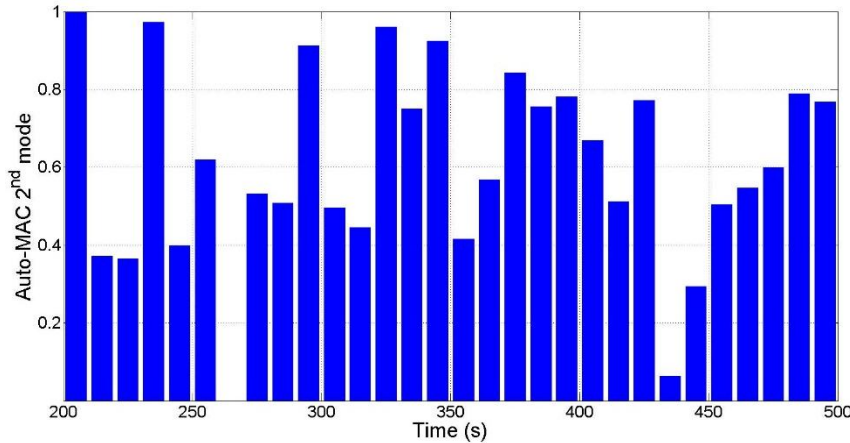
- ❑ The modes are compared with their estimation in the first time-interval
- ❑ 1st Mode shape tracking is consistent among the three flights

3. OMA on ARIANE Launch Vehicle

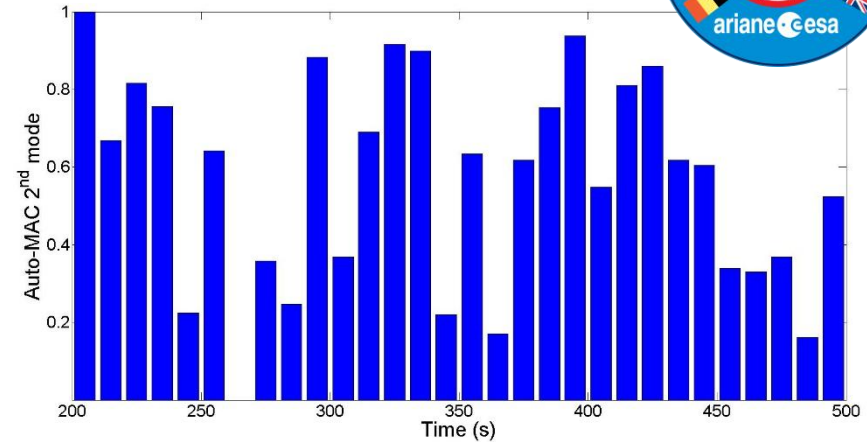


Tracking of the 2nd mode shape using FDD

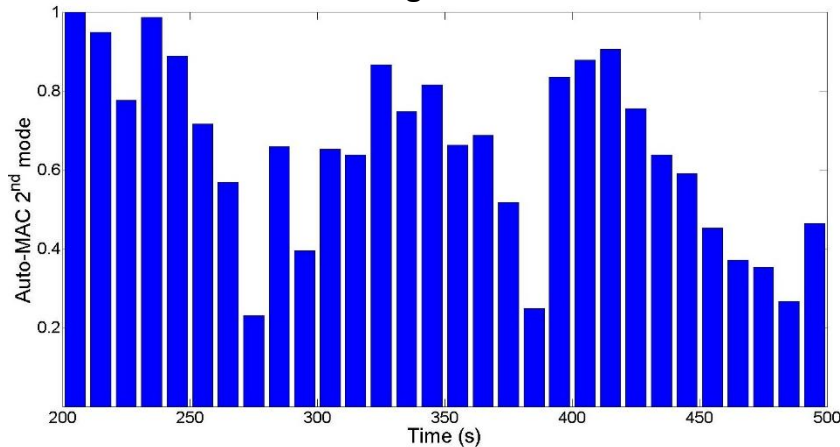
Flight#1



Flight#2



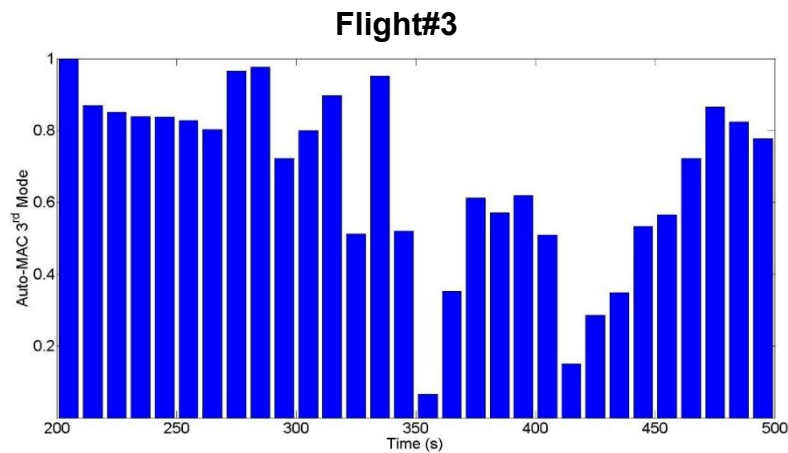
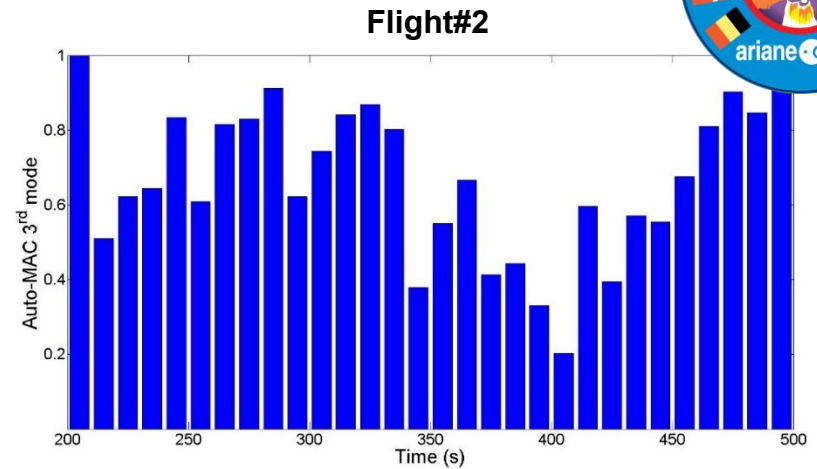
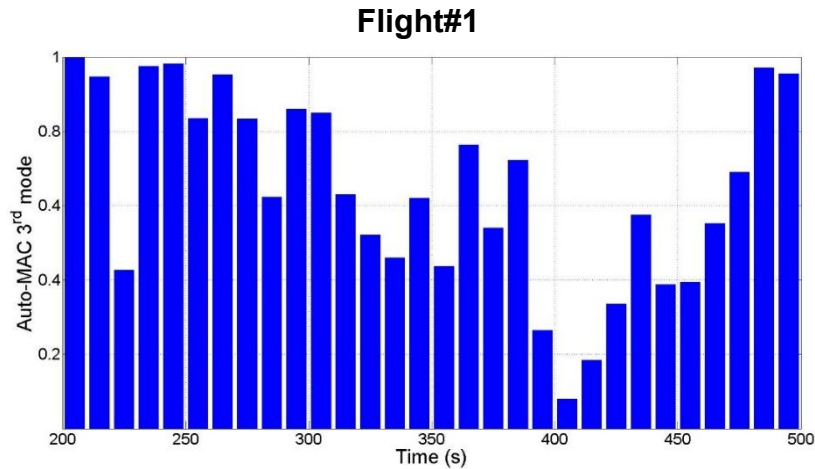
Flight#3



- The modes are compared with their estimation in the first time-interval
- 2nd Mode shape tracking is more difficult with respect the first even if the trend are consistent among the different flights (In Flight#1 and Flight#2 is not identified being not identified the frequencies)
- Not in all the time-intervals it has been possible estimate the modal parameters



Tracking of the 3rd mode shape using FDD

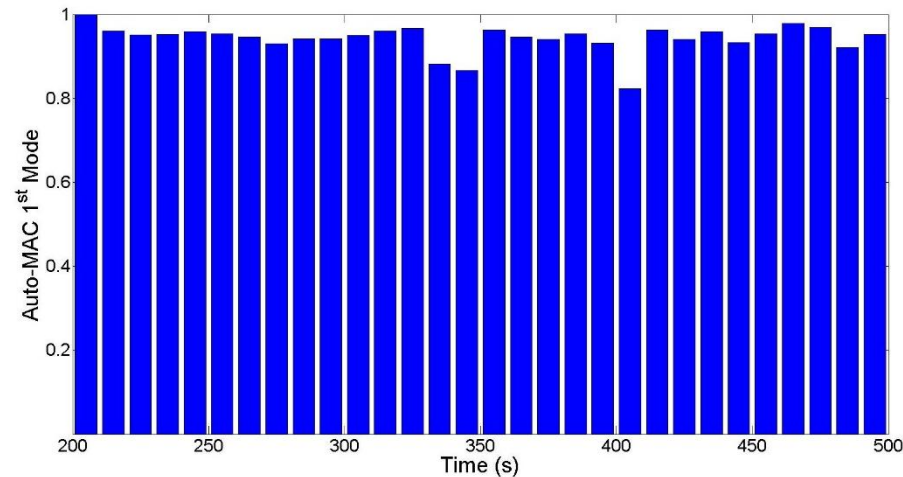
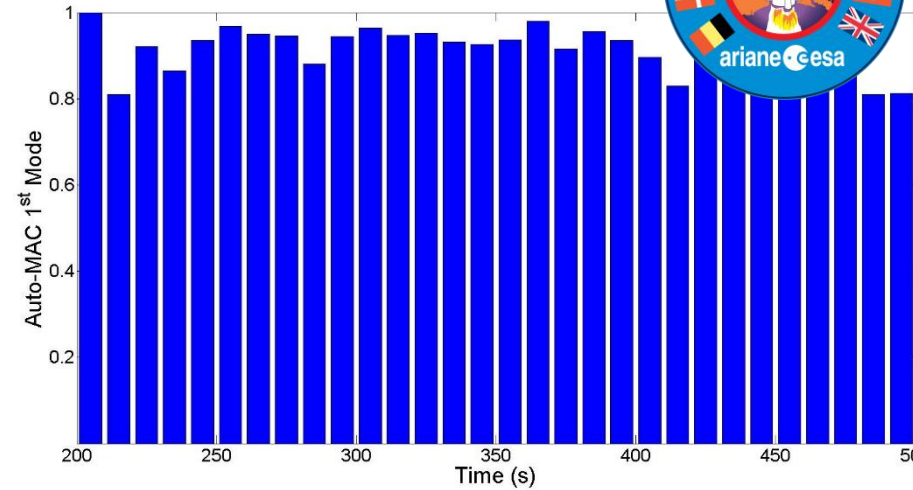
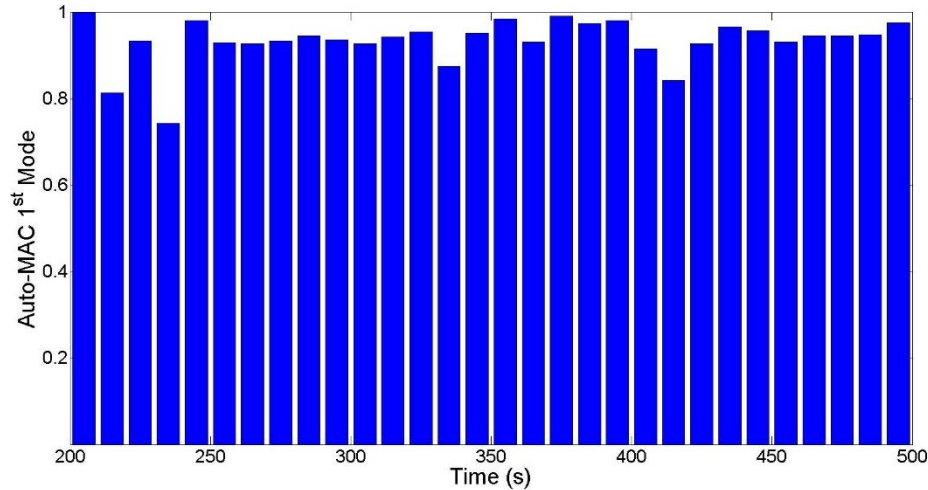


- The modes are compared with their estimation in the first time-interval
- 3rd Mode shape tracking is the most difficult with respect the first even if the trend are similar among the different flights
- Not in all the time-intervals it has been possible estimate the modal parameters

3. OMA on ARIANE Launch Vehicle



Tracking of the 1st mode shape using HTM

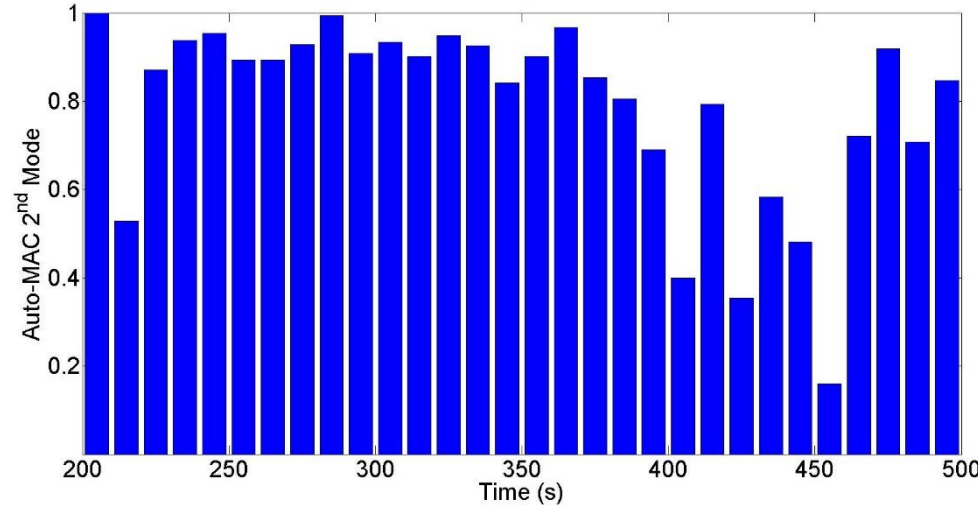
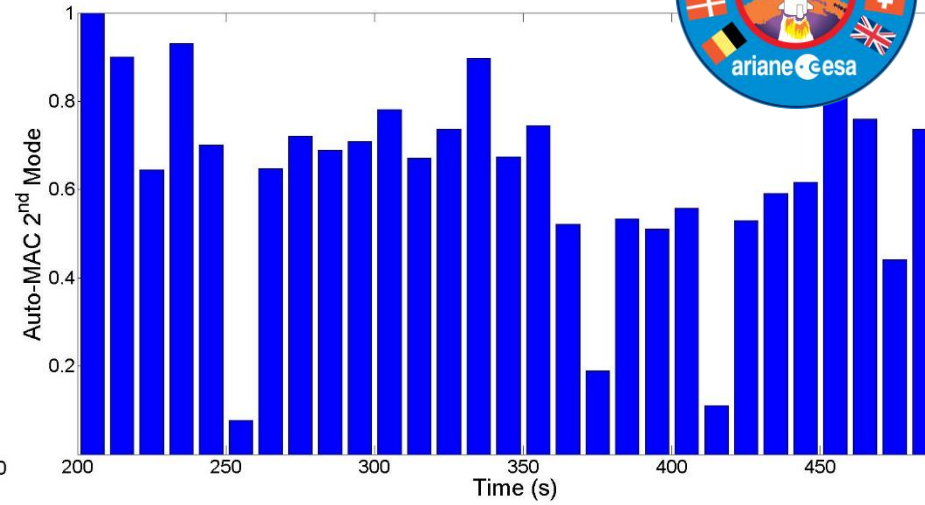
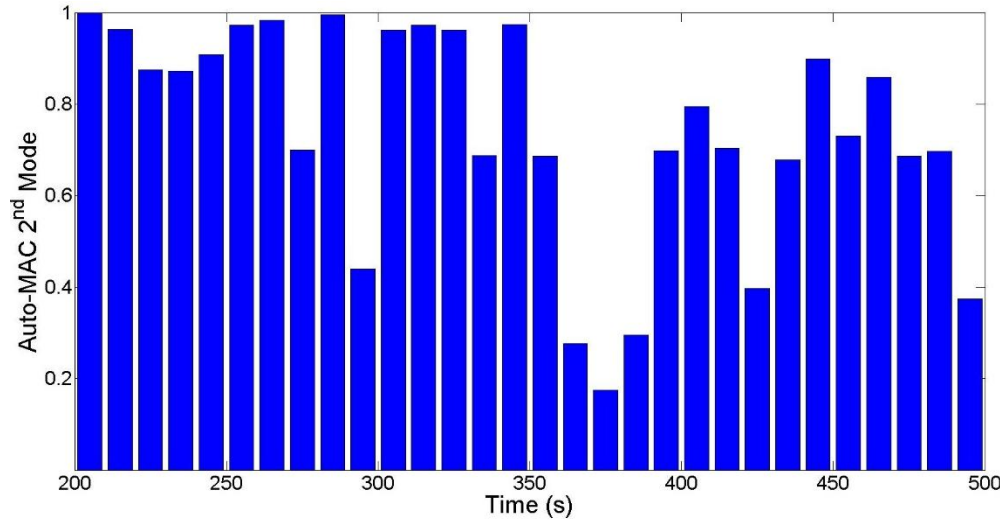


- The modes are compared with their estimation in the first time-interval
- 1st Mode shape tracking is consistent among the three flights**

3. OMA on ARIANE Launch Vehicle



Tracking of the 2nd mode shape using HTM

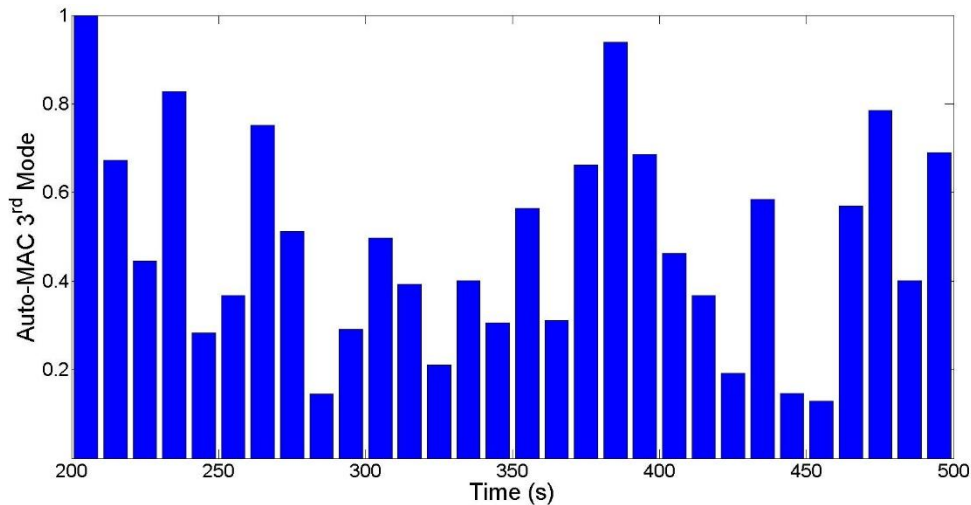
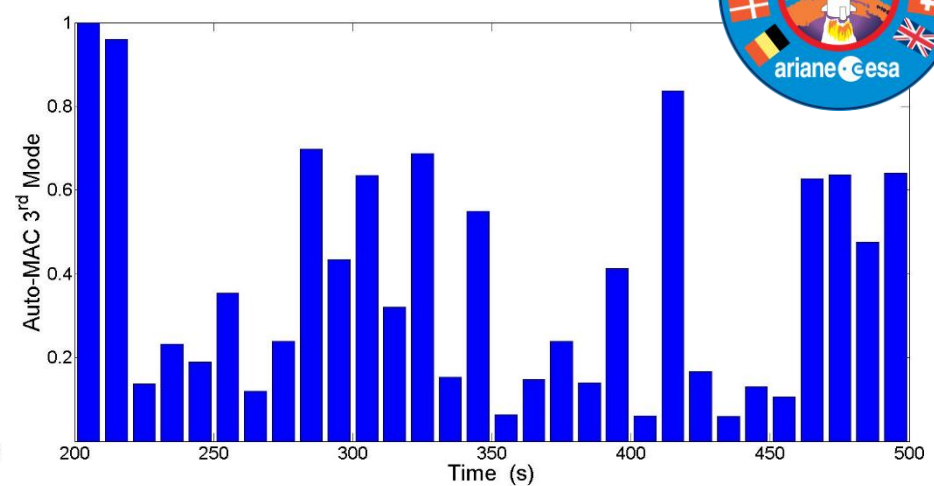
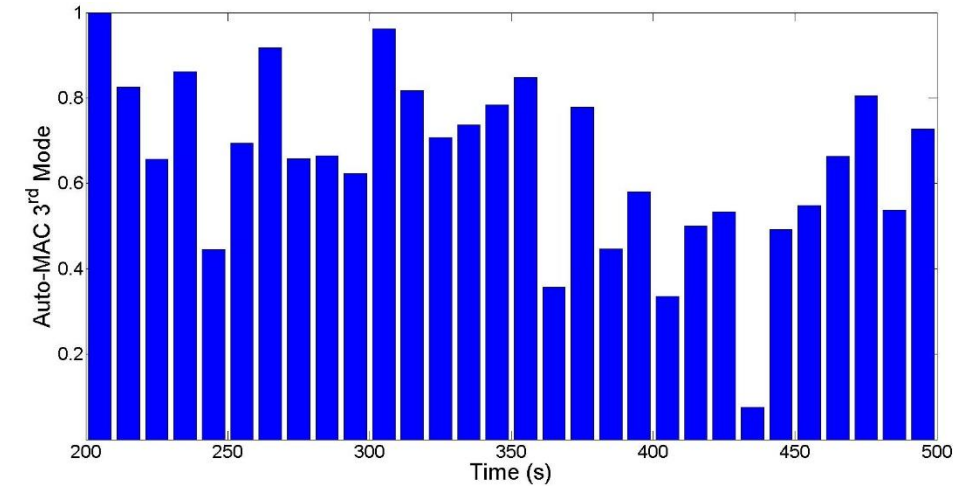


- The modes are compared with their estimation in the first time-interval
- 2nd Mode shape tracking is more difficult with respect the first even if the trend are consistent among the different flights**

3. OMA on ARIANE Launch Vehicle



Tracking of the 3rd mode shape using HTM



- The modes are compared with their estimation in the first time-interval
- 3rd Mode shape tracking is the most difficult**
- The dispersion of the estimates suggest a lack of samples for this method**

Agenda

1. Motivations
2. Theoretical Background on OMA approaches
3. OMA on ARIANE Launch Vehicle
4. OMA on VEGA P80 Motor
5. OMA on REXUS36 Sounding Rocket
6. Concluding Remarks



4. OMA on VEGA LV's P80 Motor

1/17



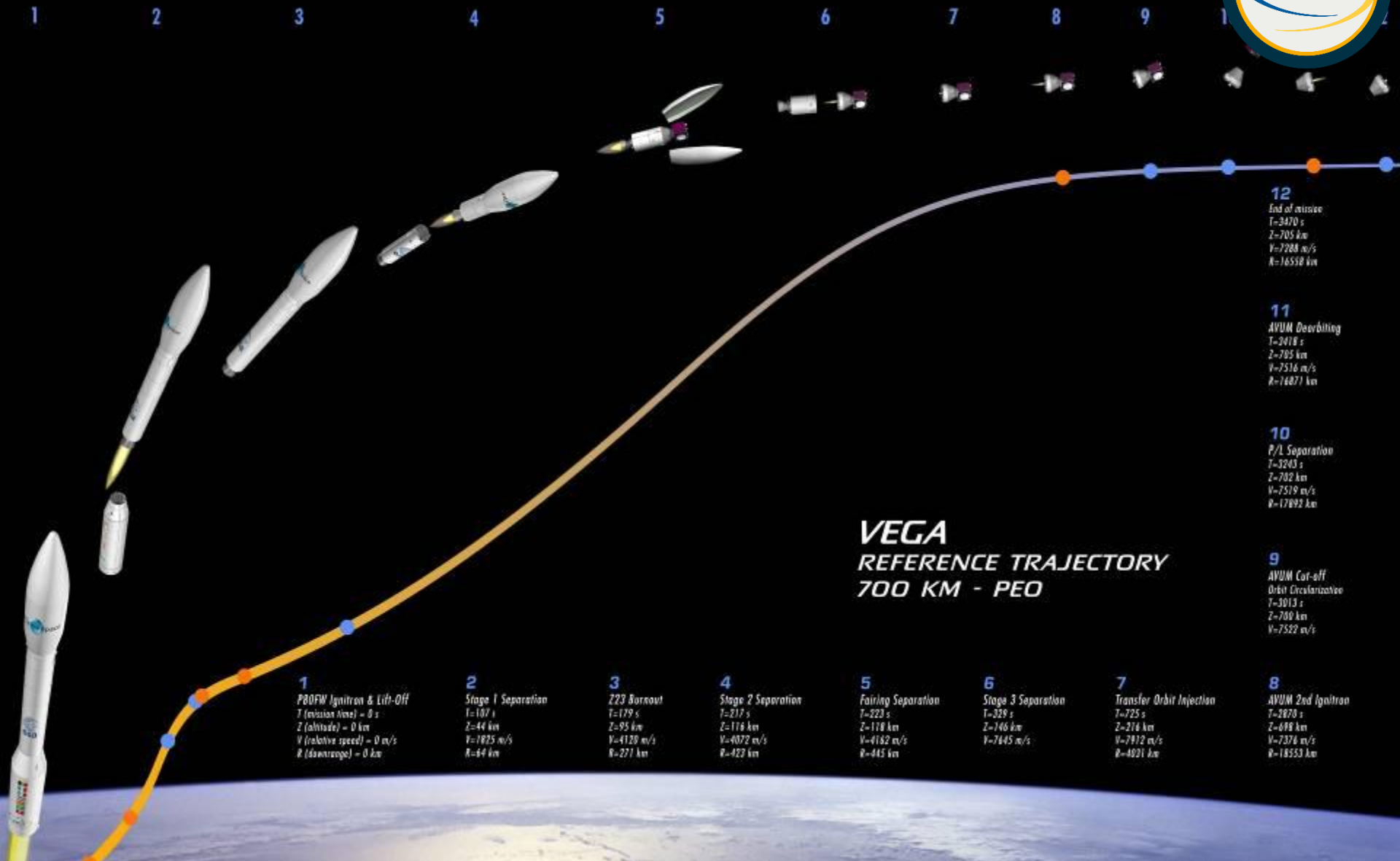
Vega is a four-stage vehicle mainly based on solid propulsion, with a high level of integration within the Ariane LV family.



Height [m]	30.152
Maximum diameter [m]	3.005
Fairing diameter [m]	2.600
Mass at Lift-off [kg]	136.811
Reference mission performance [kg]	1500

4. OMA on VEGA LV's P80 Motor

2/17



1
P80FW Ignition & Lift-Off
T (eviction time) = 0 s
Z (altitude) = 0 km
V (relative speed) = 0 m/s
R (downrange) = 0 km

2
Stage 1 Separation
T = 107 s
Z = 44 km
V = 1825 m/s
R = 64 km

3
Z23 Burnout
T = 179 s
Z = 95 km
V = 4120 m/s
R = 271 km

4
Stage 2 Separation
T = 217 s
Z = 176 km
V = 4072 m/s
R = 422 km

5
Fairing Separation
T = 223 s
Z = 178 km
V = 4162 m/s
R = 415 km

6
Stage 3 Separation
T = 329 s
Z = 746 km
V = 7645 m/s

7
Transfer Orbit Injection
T = 725 s
Z = 216 km
V = 7376 m/s
R = 4021 km

8
AVUM 2nd Ignition
T = 2870 s
Z = 698 km
V = 7376 m/s
R = 18553 km

12
End of mission
T = 2470 s
Z = 705 km
V = 7288 m/s
R = 16558 km

11
AVUM Descent
T = 2418 s
Z = 705 km
V = 7516 m/s
R = 16871 km

10
P/L Separation
T = 3243 s
Z = 702 km
V = 7519 m/s
R = 17092 km

9
AVUM Cut-off
Orbit Circularization
T = 3013 s
Z = 700 km
V = 7552 m/s

VEGA
REFERENCE TRAJECTORY
700 KM - PEO

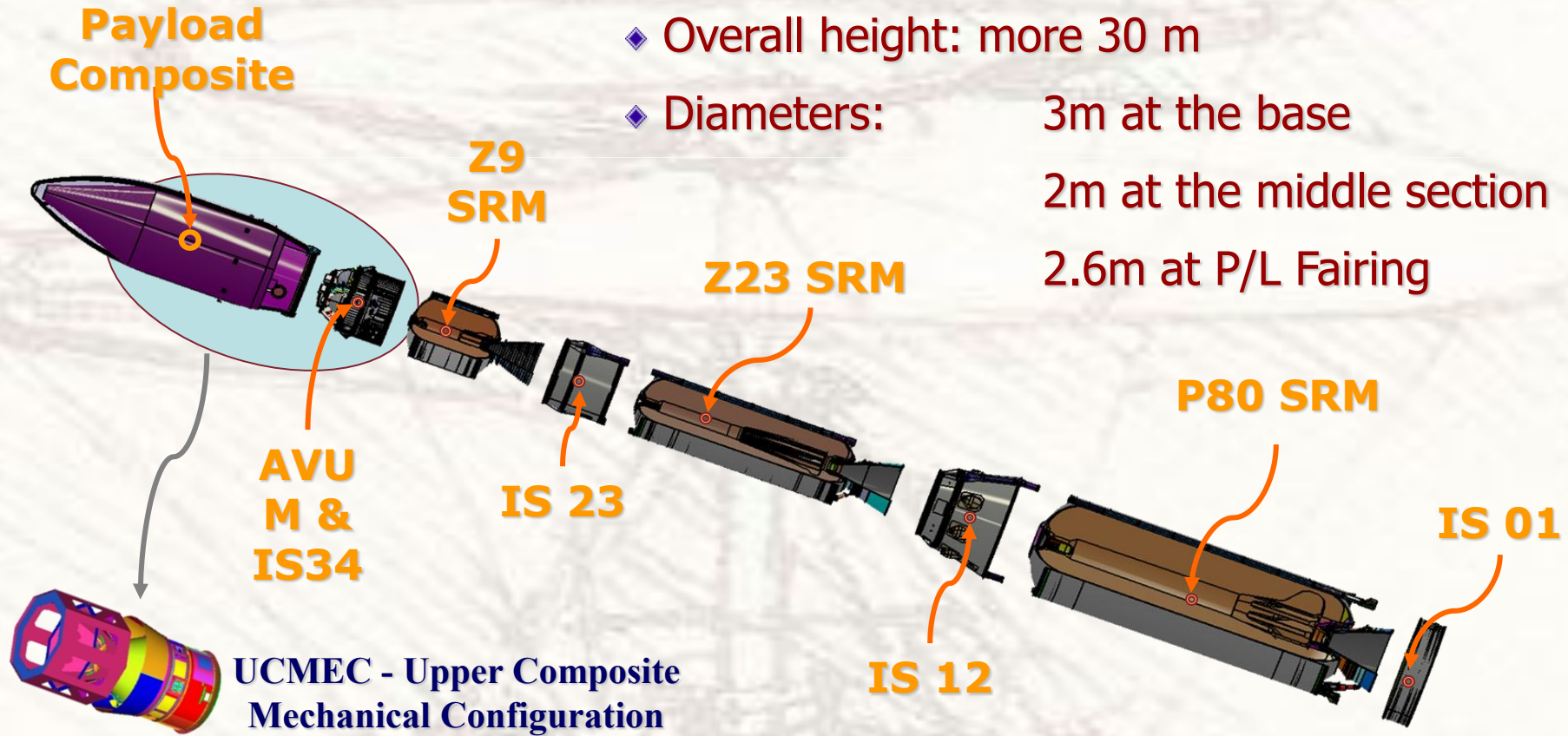
4. OMA on VEGA LV's P80 Motor

3/17



■ Axis symmetric body

- ◆ Weight at launch w/o payload: 137 t
- ◆ Overall height: more 30 m
- ◆ Diameters:
 - 3m at the base
 - 2m at the middle section
 - 2.6m at P/L Fairing

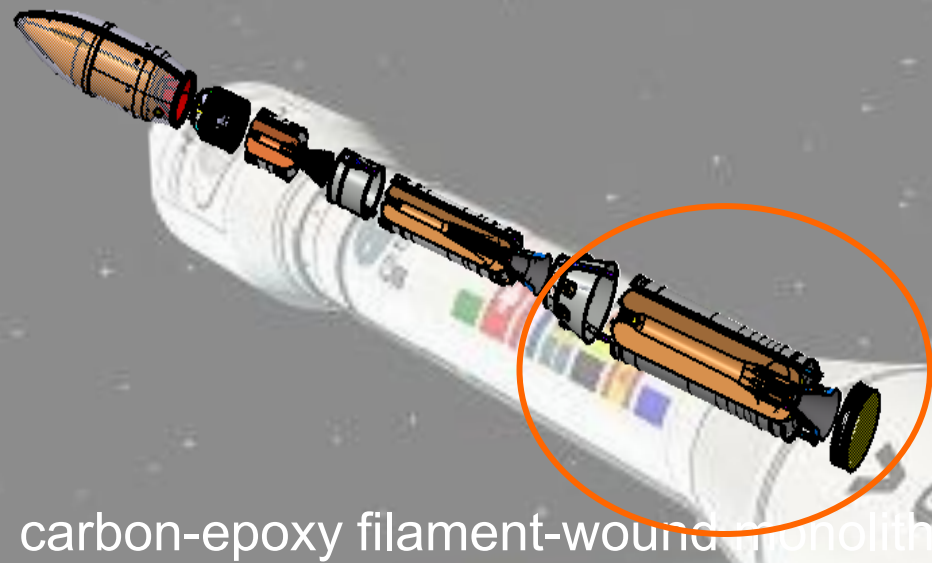


IOMAC2027 OMA Lectures: STRUCTURAL DYNAMICS EXPERIMENTS ON ESA SPACE LAUNCHERS

4. OMA on VEGA LV's P80 Motor



Length [m]	11.0
Max diameter [m]	3.0
Mass at Lift-off [kg]	97 131
Burn time [s]	106.8
Total Impulse [KN s]	242 721



carbon-epoxy filament-wound monolithic case



Retro Rocket Assy

IS 01

4. OMA on VEGA LV's P80 Motor

5/17



Firing Test at the Guyanese Space Center in Kourou

IOMAC2027 OMA Lectures: STRUCTURAL DYNAMICS EXPERIMENTS ON ESA SPACE LAUNCHERS

Dept. of Mechanical and Aerospace Engineering – University of Rome «La Sapienza», Roma, Italy
April 09, 2026

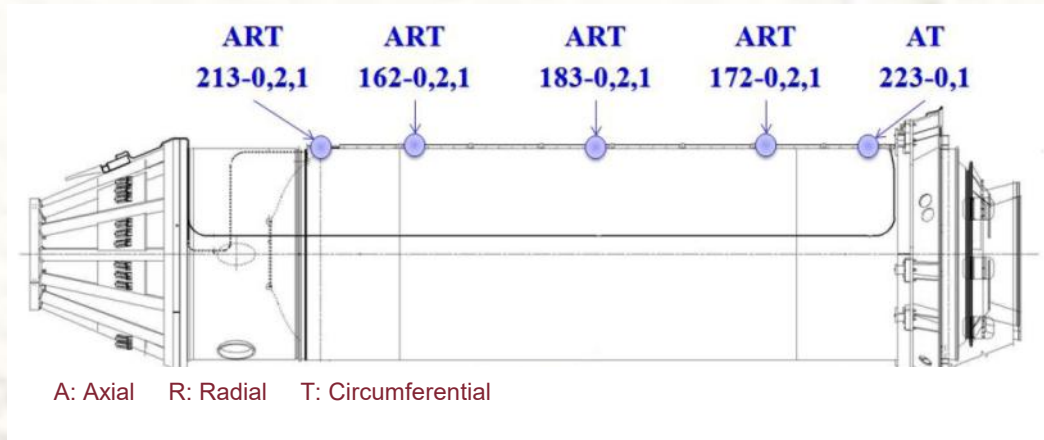
G. Coppotelli, D. Antonini, L. Onofri

4. OMA on VEGA LV's P80 Motor

7/17



Setup



Generatrix G04



Sample frequency	2500 Hz
Record time	144 s
Number of samples	359 870

Slot	30
Time	3.3 s
Samples	$2^{13}=8192$

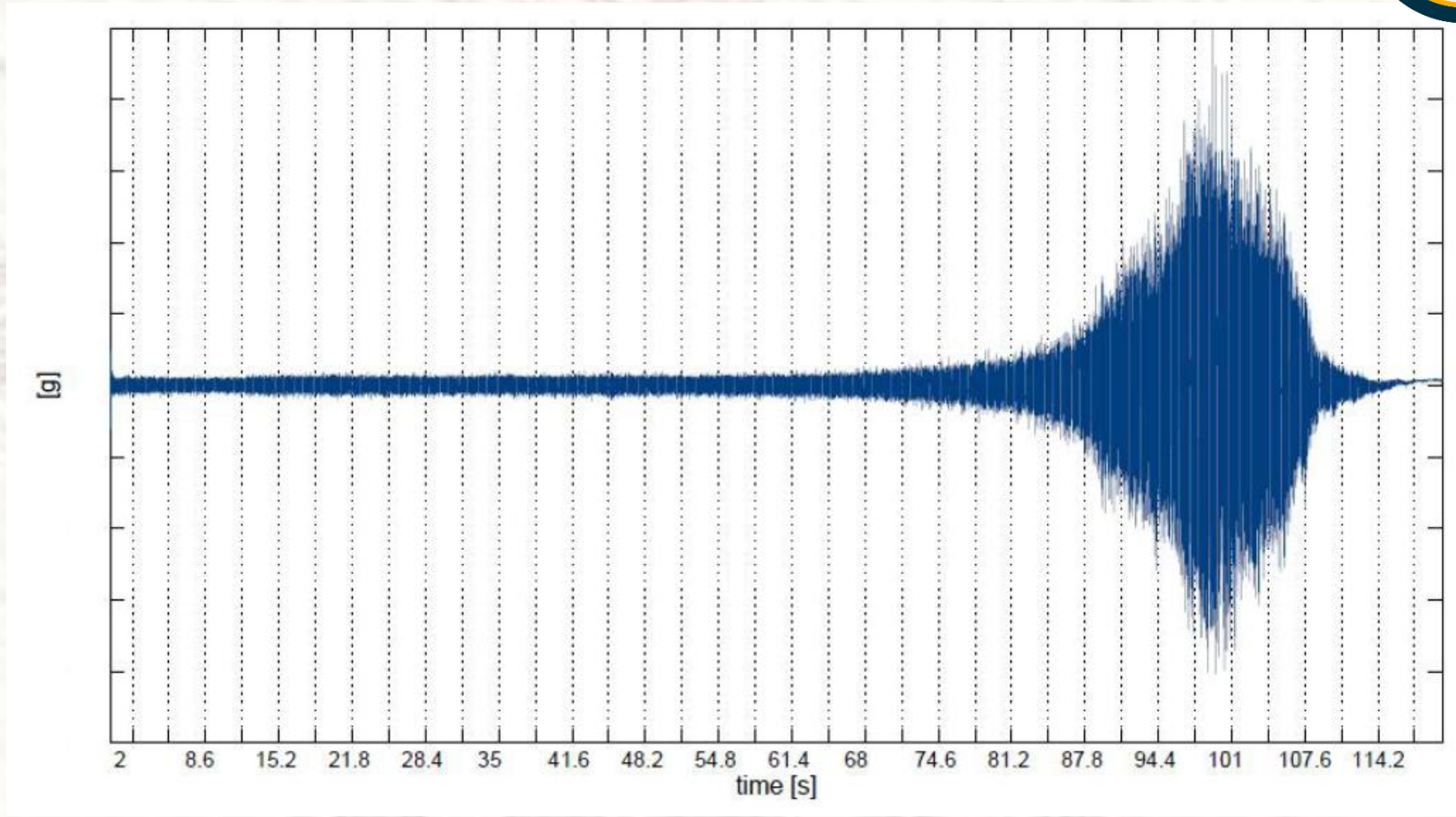
IOMAC2027 OMA Lectures: STRUCTURAL DYNAMICS EXPERIMENTS ON ESA SPACE LAUNCHERS

4. OMA on VEGA LV's P80 Motor

8/17



Accelerometer time responses



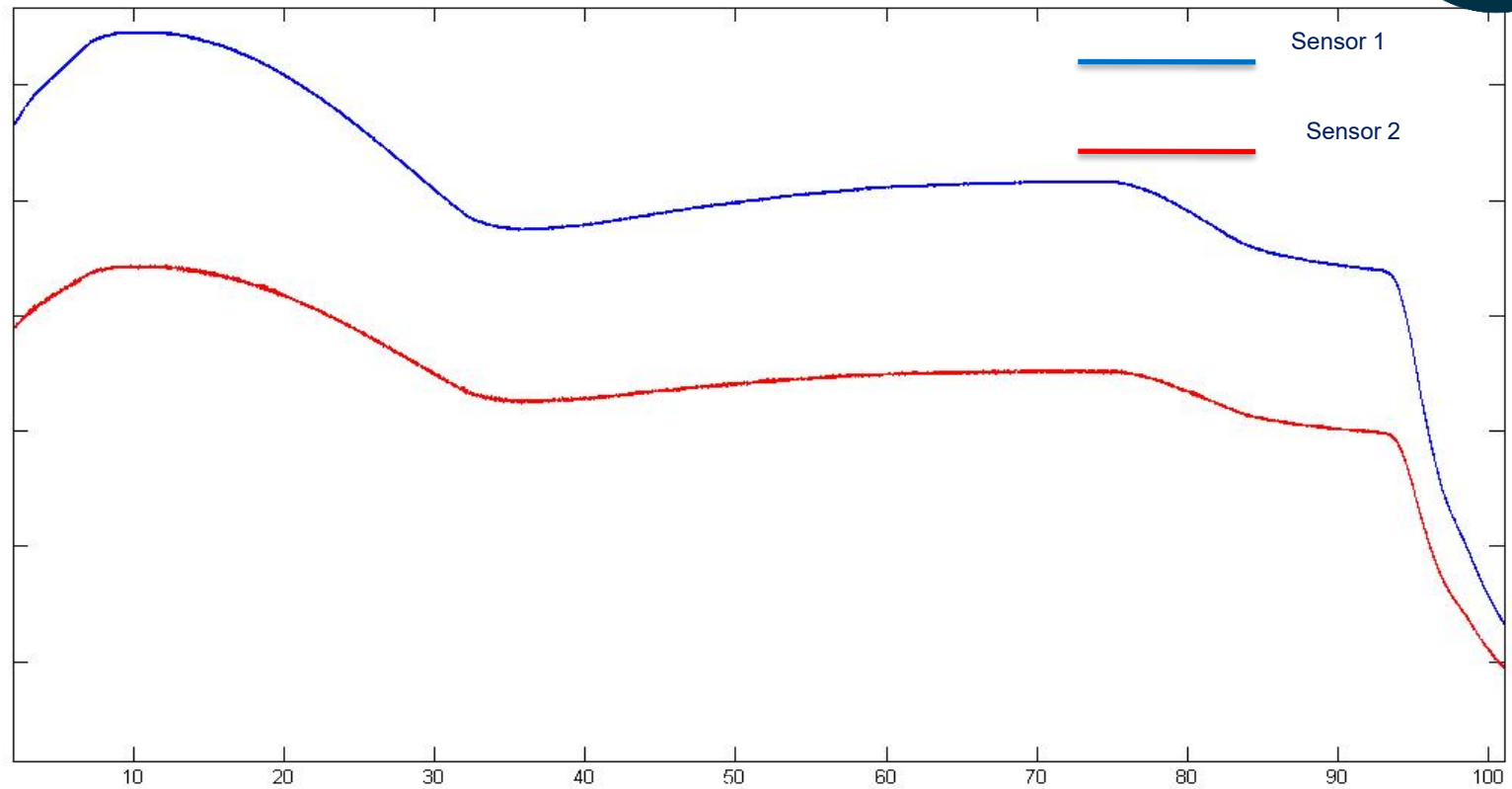
IOMAC2027 OMA Lectures: STRUCTURAL DYNAMICS EXPERIMENTS ON ESA SPACE LAUNCHERS

4. OMA on VEGA LV's P80 Motor

9/17



Strain gauge time responses

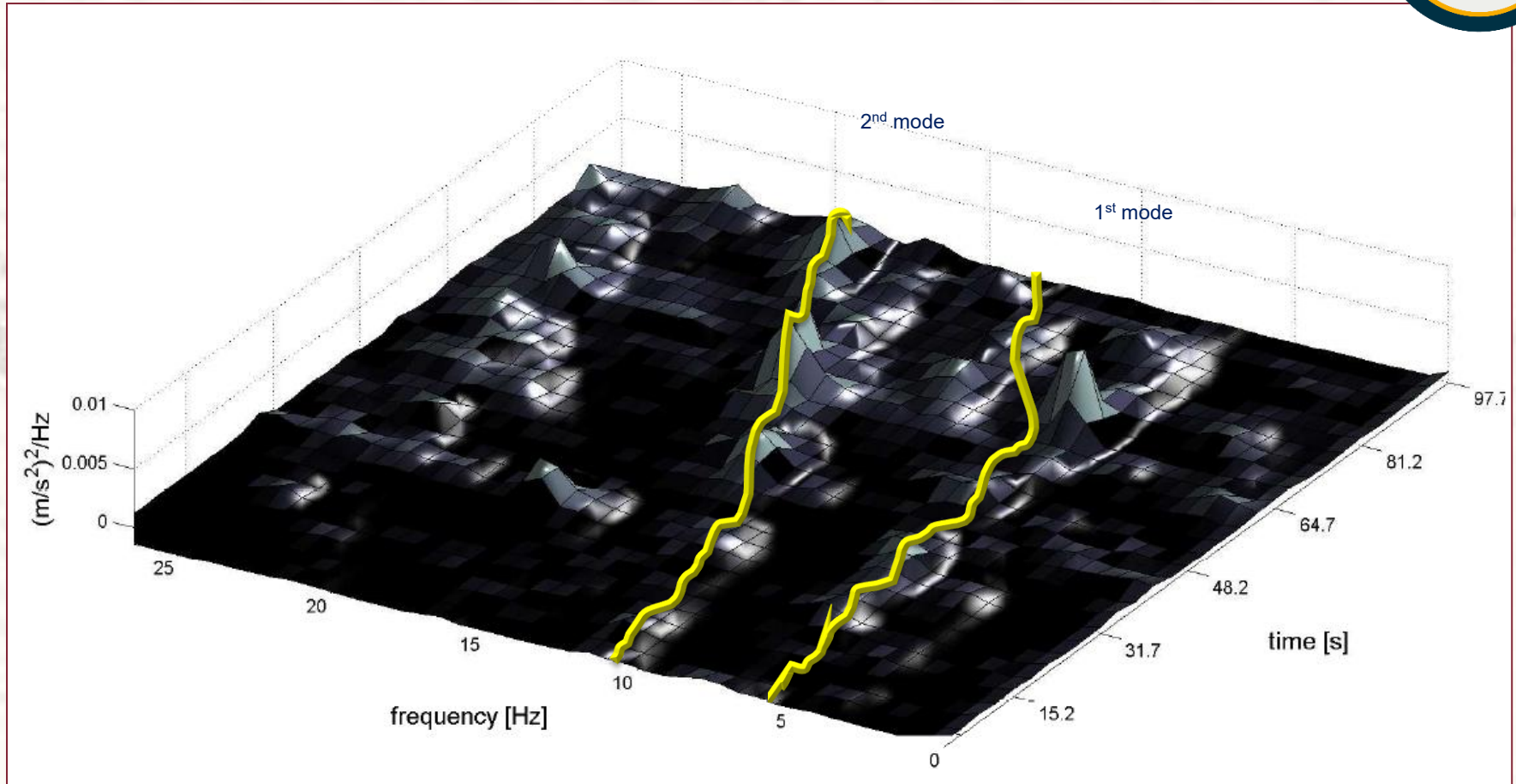


4. OMA on VEGA LV's P80 Motor

10/17



Natural Frequency tracking



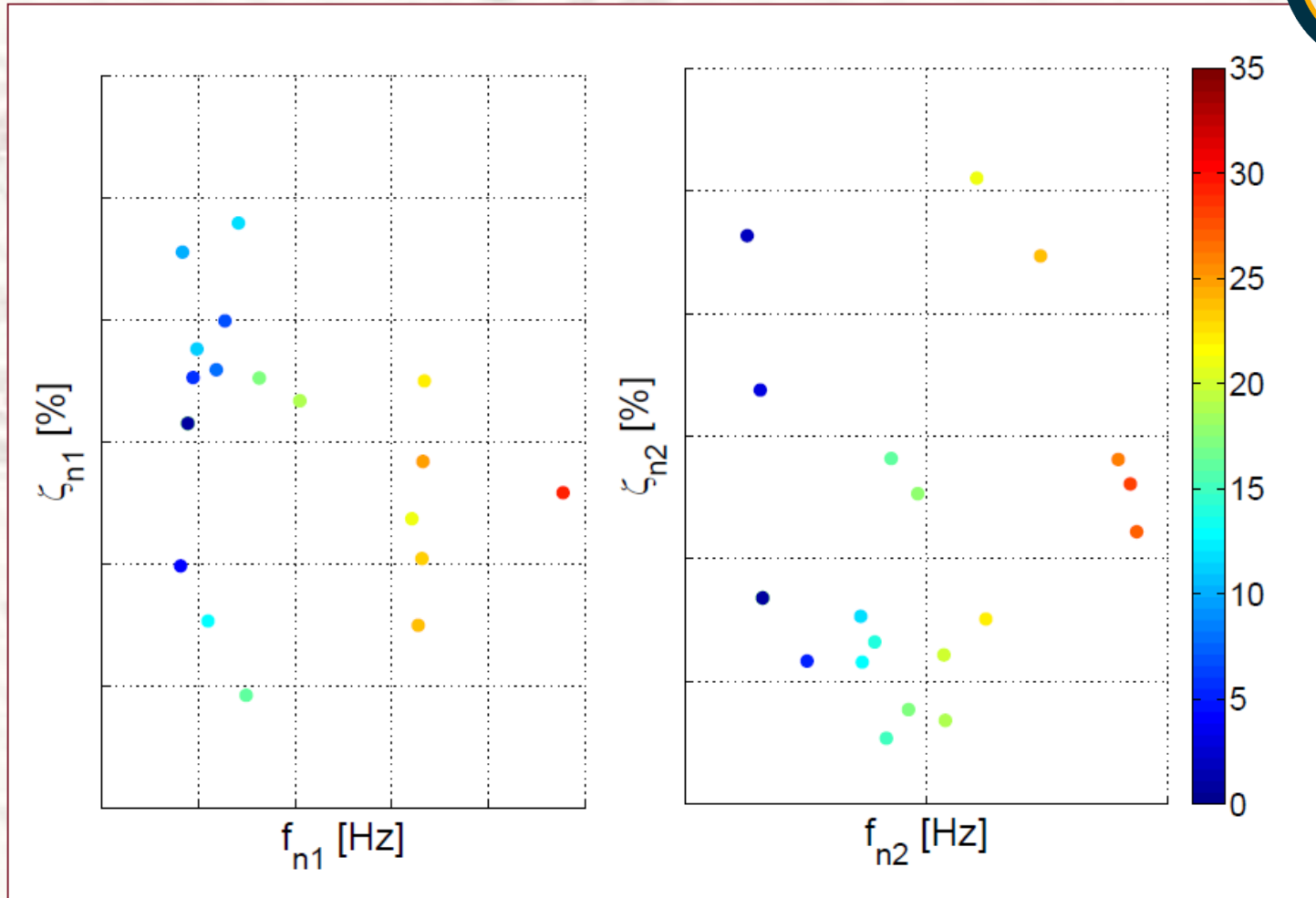
IOMAC2027 OMA Lectures: STRUCTURAL DYNAMICS EXPERIMENTS ON ESA SPACE LAUNCHERS

4. OMA on VEGA LV's P80 Motor

11/17



Root locus

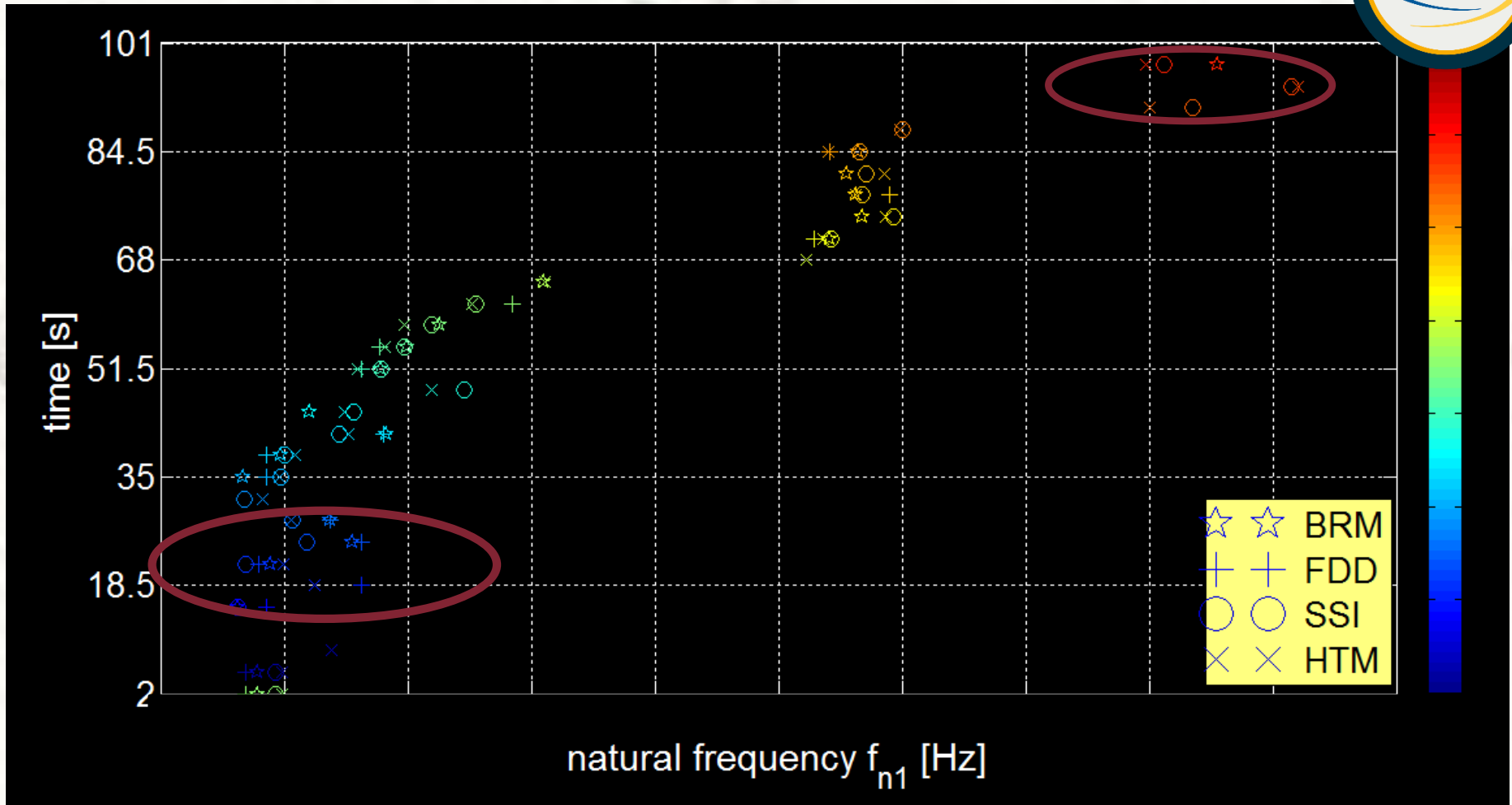


IOMAC2027 OMA Lectures: STRUCTURAL DYNAMICS EXPERIMENTS ON ESA SPACE LAUNCHERS

4. OMA on VEGA LV's P80 Motor



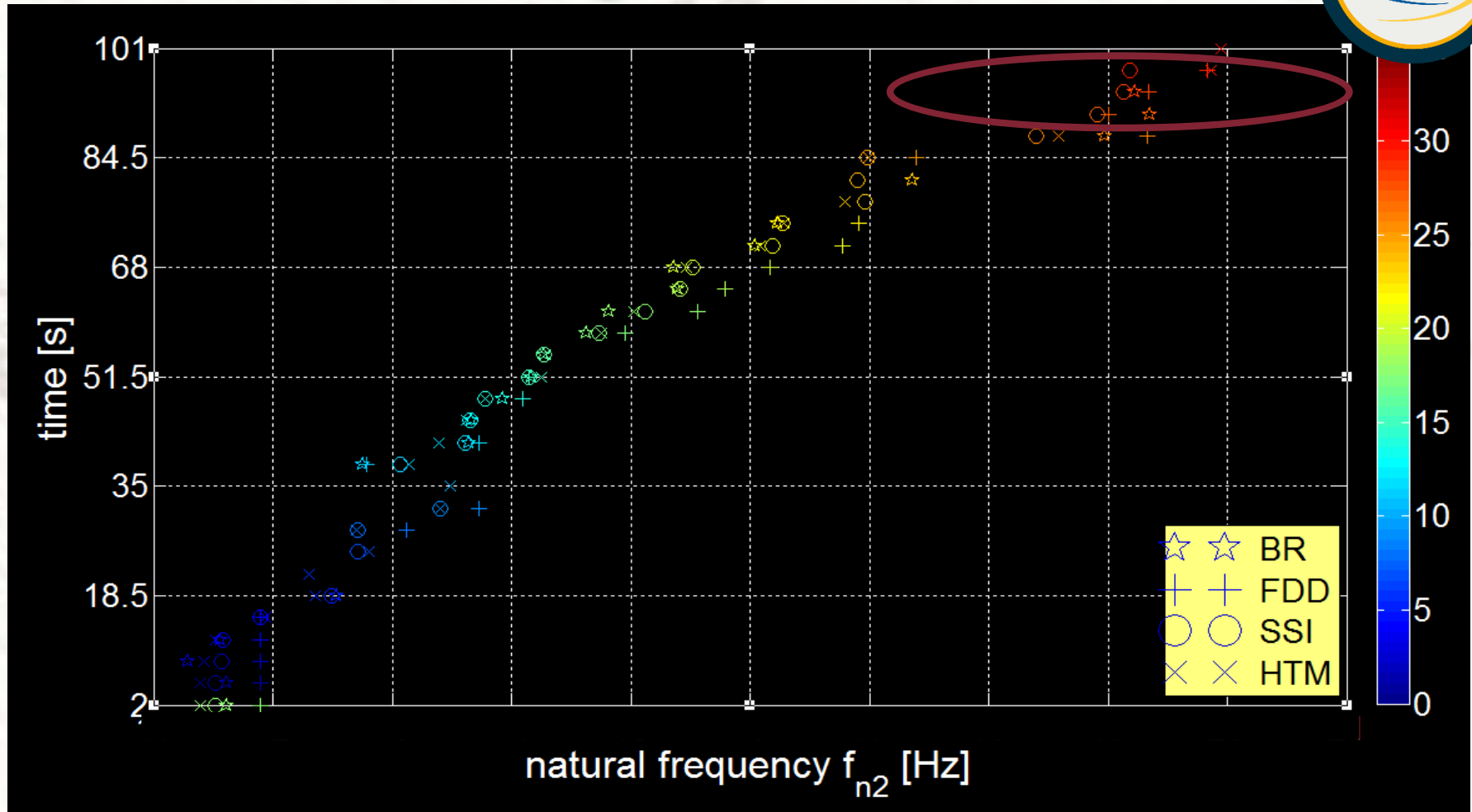
Natural frequency shift of the 1st mode:



4. OMA on VEGA LV's P80 Motor



Natural frequency shift of the 2nd mode:

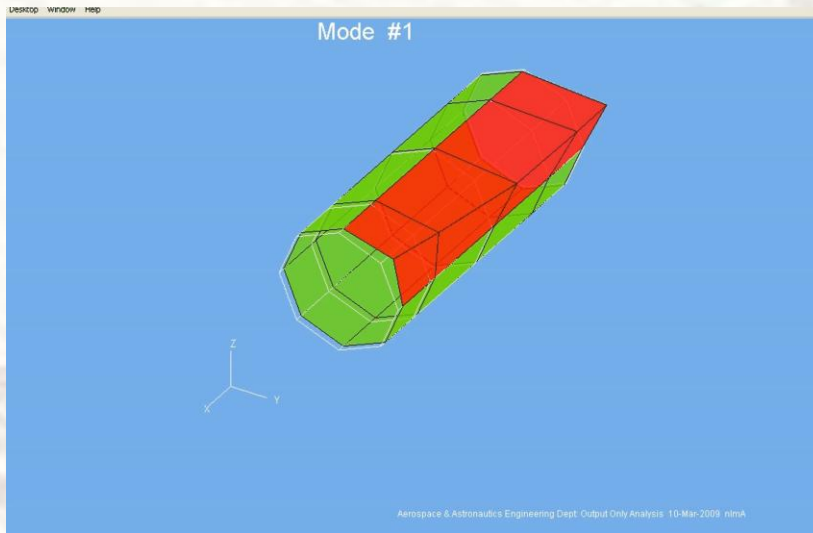


4. OMA on VEGA LV's P80 Motor

14/17



Lateral Mode



Axial Mode



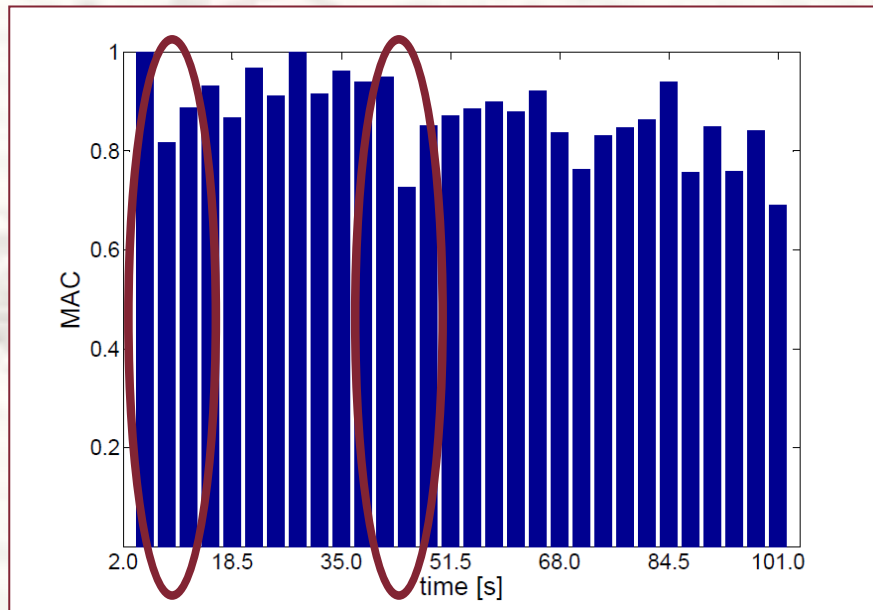
During the firing test the natural frequencies increase:

- of 138% for the lateral mode
- of 79% for the axial mode

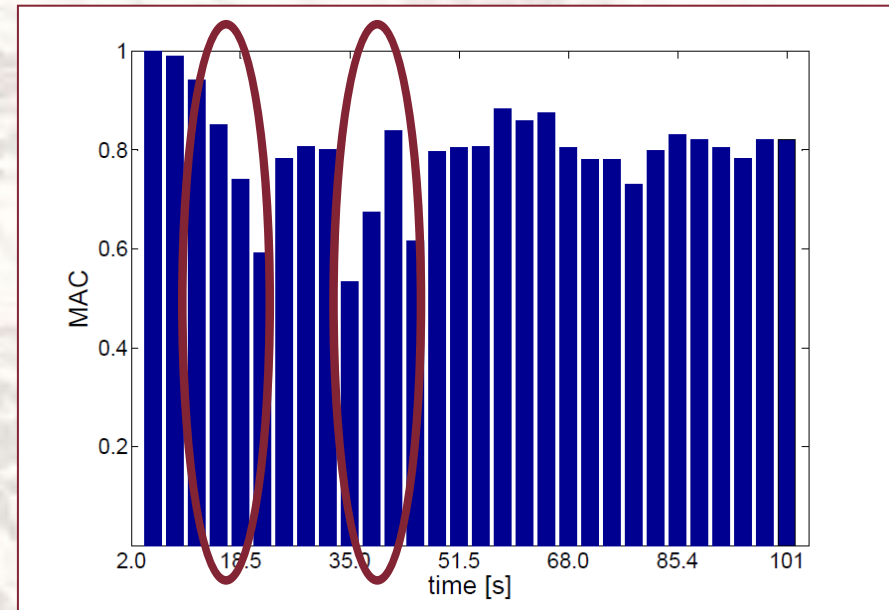
4. OMA on VEGA LV's P80 Motor



Mode shape variation:



Lateral Mode



Axial Mode

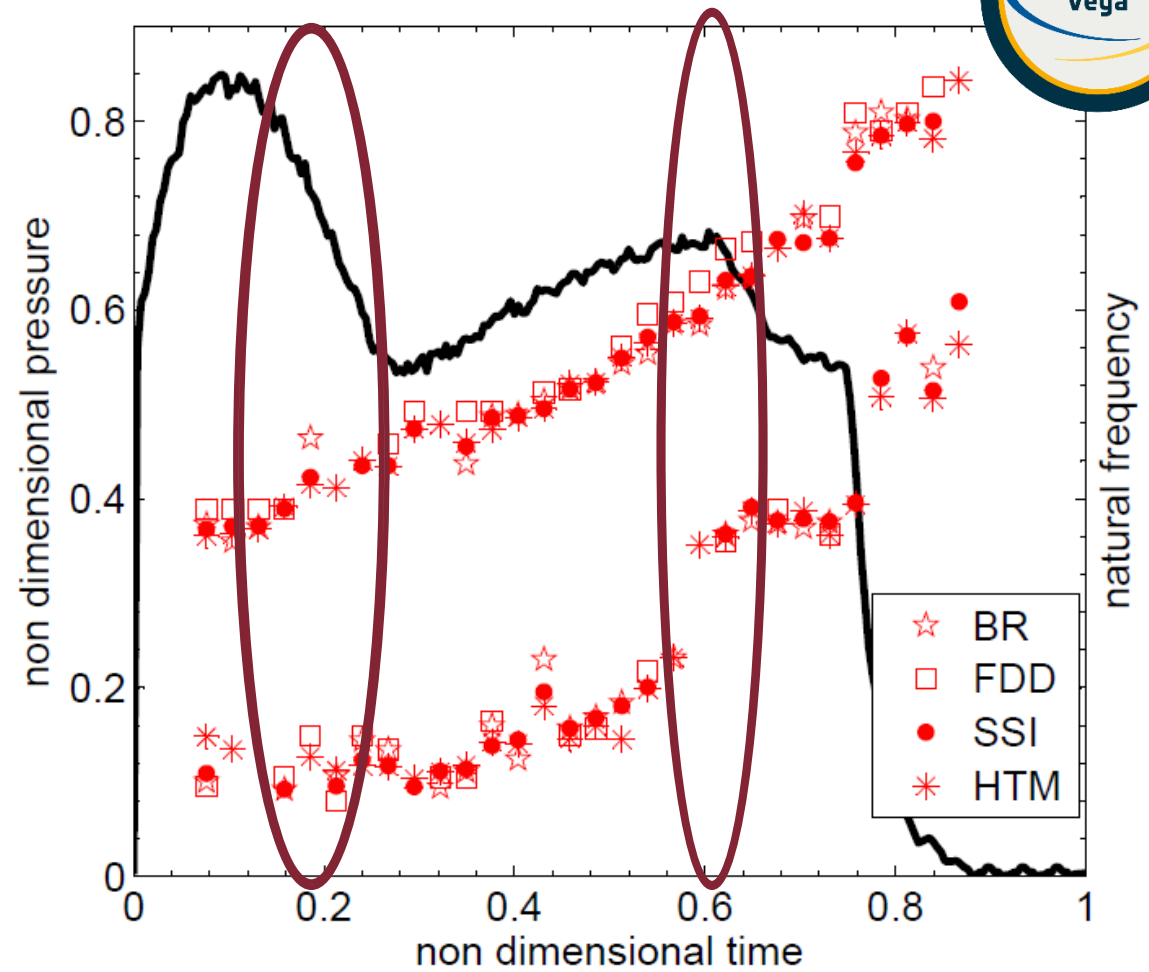
4. OMA on VEGA LV's P80 Motor

16/17



Time evolution:

- head-end pressure
- natural frequencies



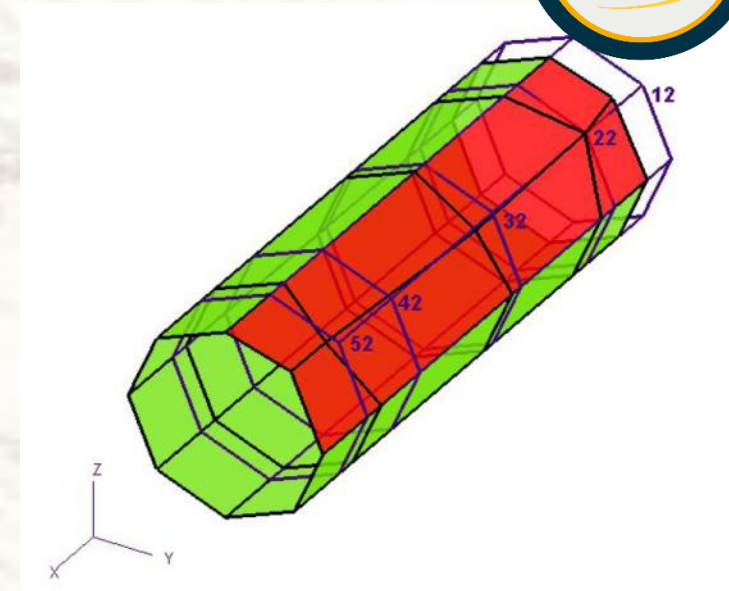
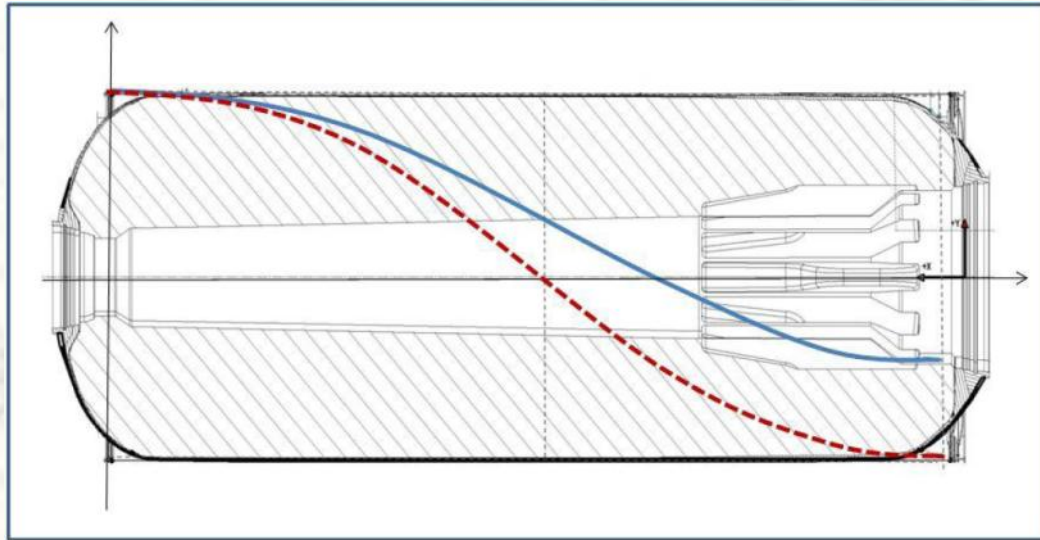
E. Cavallini, B. Favini, M. Di Giacinto, SRM Q1D Unsteady Internal Ballistic Simulation Using 3D Grain Burnback, Space Propulsion, San Sebastian, ES (2010)

4. OMA on VEGA LV's P80 Motor

17/17

1st Acoustic Mode of the combustion chamber

Operational



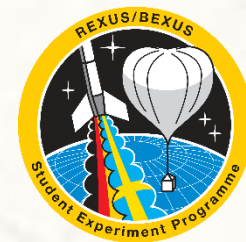
Bouffée	B0	B1	B2	B3
frequency [Hz]	50.30 – 51.50	51.50 – 51.90	53.70 – 55.00	55.10 – 55.90
damping ratio [%]	0.04 – 1.00	0.04 – 0.80	0.03 – 1.30	0.60 – 1.60

F. Mastroddi, G. Coppotelli, G.M. Polli, C. Di Trapani, Vibro-Acoustic Response Analysis to Pressure Oscillations in a Solid Rocket Motor - Comparison with the Experimental Fire-Test Data, *Aerotecnica Missili e Spazio*, ISSN 0365-7442, (2007)

IOMAC2027 OMA Lectures: STRUCTURAL DYNAMICS EXPERIMENTS ON ESA SPACE LAUNCHERS

Agenda

1. Motivations
2. Theoretical Background on OMA approaches
3. OMA on ARIANE Launch Vehicle
4. OMA on VEGA P80 Motor
5. OMA on REXUS36 Sounding Rocket
6. Concluding Remarks



5. OMA on REXUS36 Sounding Rocket

1/40



SAPIENZA
UNIVERSITÀ DI ROMA



VIPER

Vibro-mechanical and Inertial
Positioning Experiment on Rocket

The VIPER mission, selected for launch on board the Improved Orion suborbital rocket, is scheduled to fly in March 2026 within the context of the European Space Agency's REXUS/BEXUS programme. The mission, entirely developed by master's and PhD students at Sapienza University of Rome, will feature two different experiments which aim to better characterize our understanding of flight vehicle structural dynamics and the effect of the launch vehicle environment on small payloads.

The first experiment, dedicated to dynamic system characterization, focuses on the analysis of the variation of modal frequencies and mode shapes of the REXUS launch vehicle throughout its flight envelope. Accordingly, the launcher dynamics during re-entry will also be observed to further improve our understanding of the modal behavior of the system during this phase.

The second experiment is focused on developing vibration mitigation strategies for payload systems. The objective of the experiment is to identify and validate effective solutions for minimizing vibrational loads transmitted to payloads by testing innovative materials and optimized structural junctions.



IOMAC2027 OMA Lectures: STRUCTURAL DYNAMICS EXPERIMENTS ON ESA SPACE LAUNCHERS

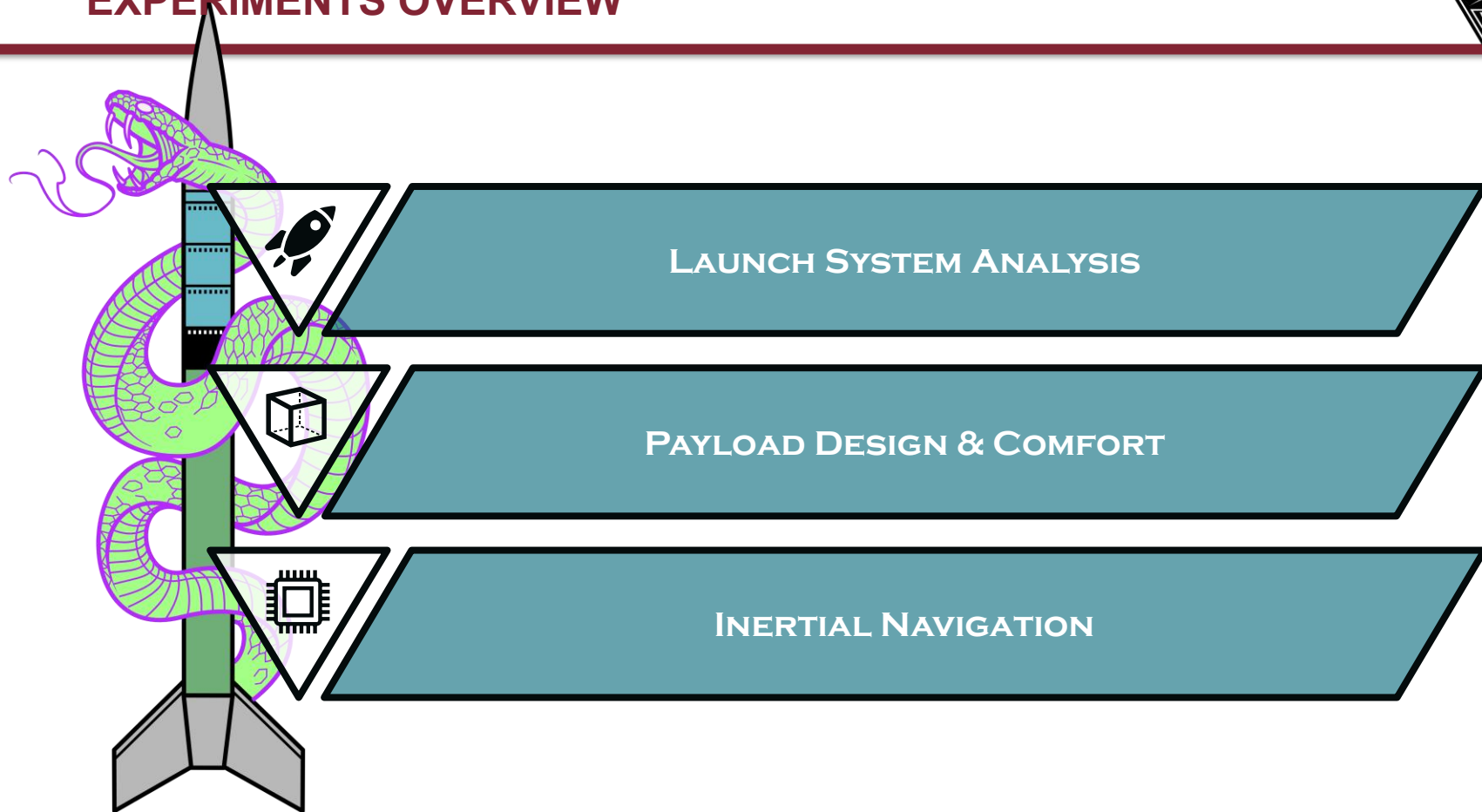
Dept. of Mechanical and Aerospace Engineering – University of Rome «La Sapienza», Roma, Italy
April 09, 2026

5. OMA on REXUS36 Sounding Rocket

2/40



EXPERIMENTS OVERVIEW



IOMAC2027 OMA Lectures: STRUCTURAL DYNAMICS EXPERIMENTS ON ESA SPACE LAUNCHERS

5. OMA on REXUS36 Sounding Rocket

3/40



MAIN SPONSORS

SIEMENS

 **PCB PIEZOTRONICS**
AN AMPHENOL COMPANY

 **RMIT**
UNIVERSITY

 **ROMA**
CAPITALE

IOMAC2027 OMA Lectures: STRUCTURAL DYNAMICS EXPERIMENTS ON ESA SPACE LAUNCHERS

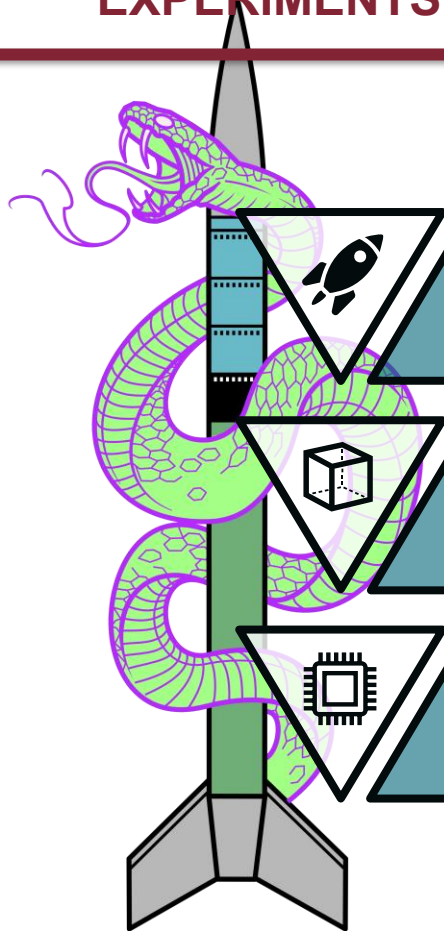
Dept. of Mechanical and Aerospace Engineering – University of Rome «La Sapienza», Roma, Italy
April 09, 2026

5. OMA on REXUS36 Sounding Rocket

4/40



EXPERIMENTS OVERVIEW



To **measure** the **time variation** of the **modal properties** of the *launch vehicle* during the whole flight.

To **assess** how **different materials** and **junctions** impact a *CubeSat's structural response* and *payload insulation* during launch vibrations, while **evaluating** operational performance under **minor controlled damage**.

To **test** and **validate** the **performance** of **real-time Inertial Navigation Systems** for *launch vehicles*, and to study the benefits of multiple distributed sensors and their optimal location along the launch vehicle.

5. OMA on REXUS36 Sounding Rocket

5/40



TIME VARIATION OF THE LAUNCHER MODAL PROPERTIES



EXPERIMENT COMPONENTS



SCADAS XS



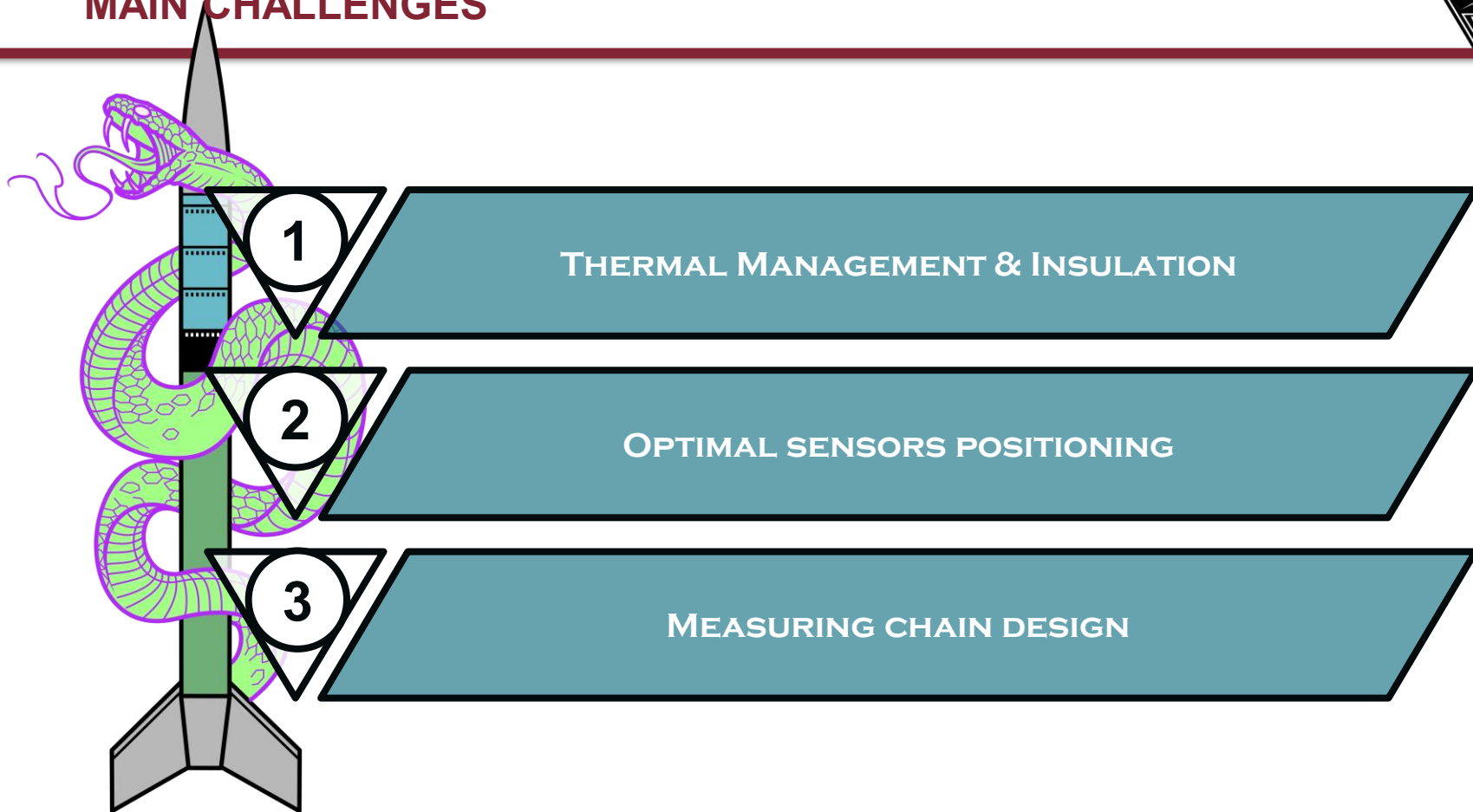
X 11 ACCELEROMETERS

5. OMA on REXUS36 Sounding Rocket

6/40



MAIN CHALLENGES



IOMAC2027 OMA Lectures: STRUCTURAL DYNAMICS EXPERIMENTS ON ESA SPACE LAUNCHERS

5. OMA on REXUS36 Sounding Rocket

7/40



THERMAL MANAGEMENT & INSULATION

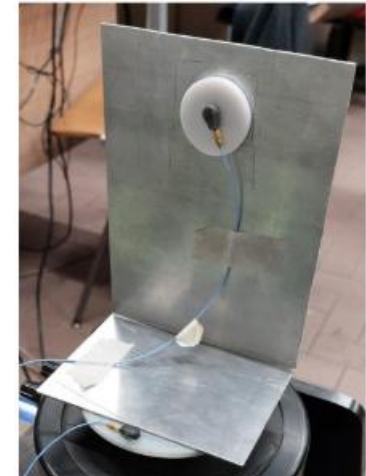
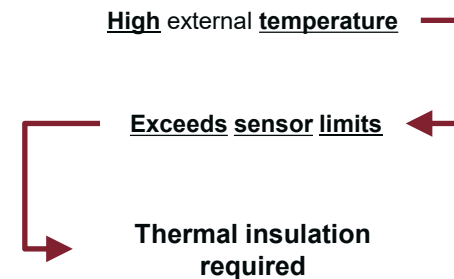
ACCELEROMETERS MOUNTING CHALLENGE

Thermal design for the VIPER experiment is mainly focused on the **launcher mounted sensors**, as they will experience the **highest temperature changes** given by the **conductive heat transfer** of the **launcher structure**

Component	Name	Operating Temp (° C)		Nosecone Placement
		Min	Max	
Rocket Structure Accelerometers	PCB Electronics ICP352C22	-54	121	Yes

NOSECONE OUTSIDE TEMPERATURE UP TO 200 C°

The temperature outside is higher than the maximum operating temperature of the accelerometers, thus a thermal insulation device is required.



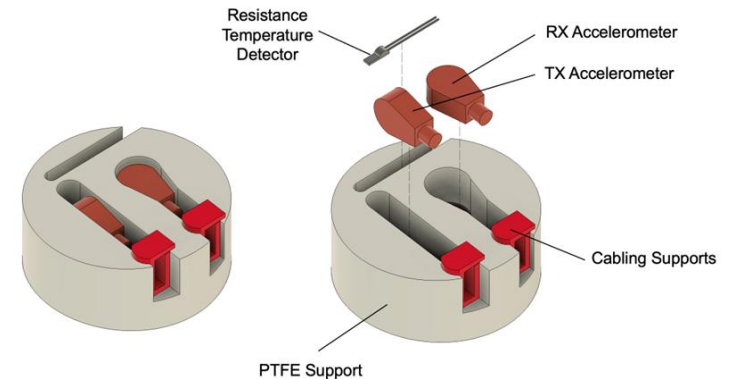


THERMAL MANAGEMENT & INSULATION

DESIGN

To choose the material and thickness of the insulation layer different choices were taken into account. Important features to take into account are:

	MATERIAL	
	PEEK	PTFE
DENSITY	1.3 - 1.32	2.1 - 2.2
YOUNG MODULUS	3.3 - 4.0	0.5
GLASS-TRANSITION TEMPERATURE	143	100
THERMAL CONDUCTIVITY	0.25	0.25



- Thermal insulation was bonded to the module inner wall using 3M™ VHB™ F9473PC high-temperature adhesive tape.
- Performance was validated through testing with a PTFE support plate, integrating an RTD sensor for temperature monitoring.
- A 1D transient thermal analysis was conducted to define the required insulation thickness, ensuring temperatures remain within sensor operating limits.



THERMAL MANAGEMENT & INSULATION

TESTING

Thermal and vibro-thermal on the PTFE supports shown their viability as insulation material. On the other hand, the glass-transition temperature was considered too low for the mission, therefore PEEK was chosen.

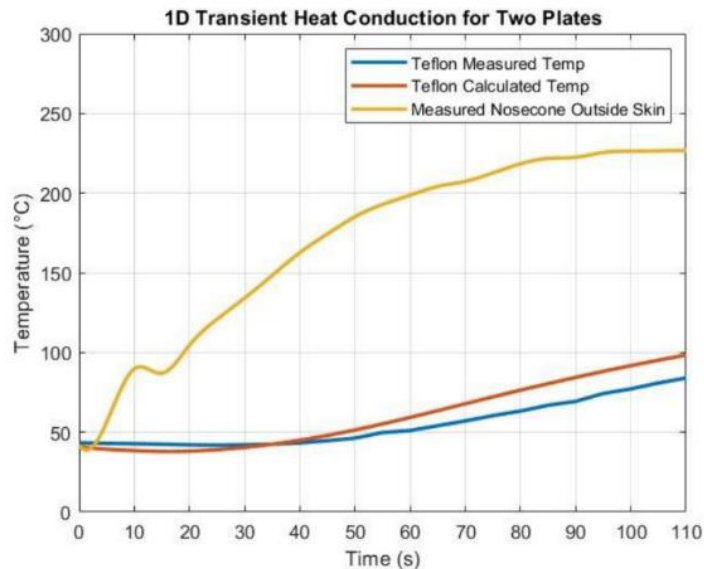
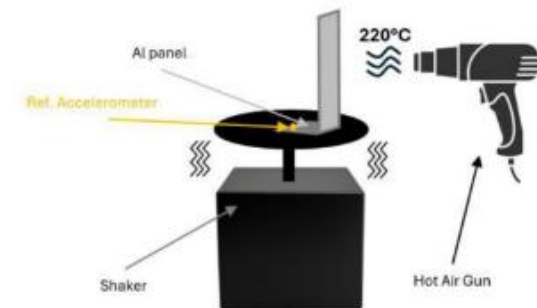
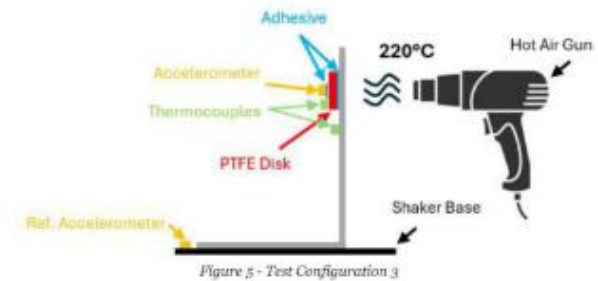


Figure 10 - Thermo-Vibrational Test Temperature Profile

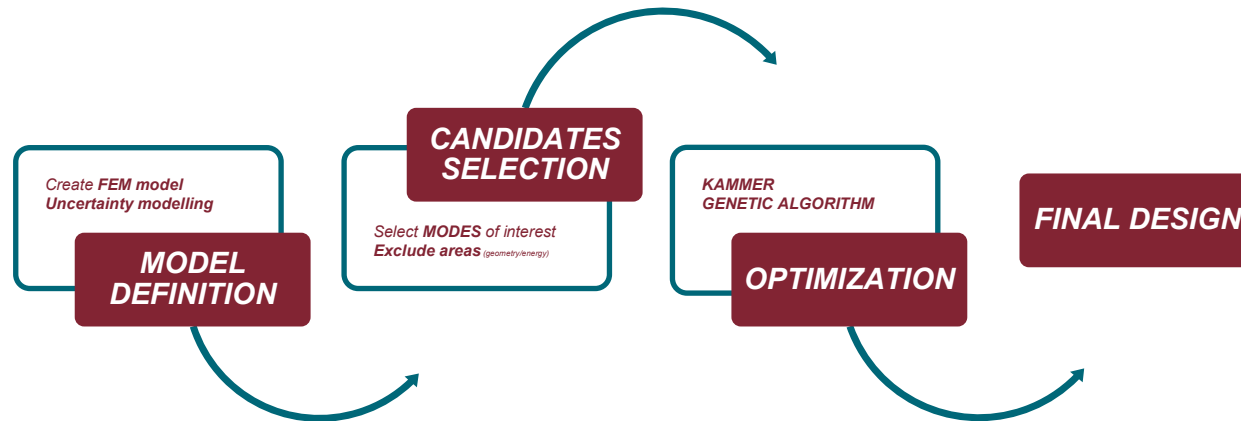




OPTIMAL SENSOR POSITIONING

OBJECTIVES

- ✓ **Maximize information** content
- ✓ Achieve **robust** and **reliable** sensor **placement**
- ✓ **Mitigate noise** and **modeling uncertainties**



KAMMER: quicker, low computational cost, easy to implement, limited flexibility in handling complex geometrical constraints

GENETIC ALGORITHM: strong constraint-handling capabilities, global search, suitable for complex layouts

5. OMA on REXUS36 Sounding Rocket

11/40



OPTIMAL SENSOR POSITIONING

DATA PRE-PROCESSING: *Nodes to be excluded*

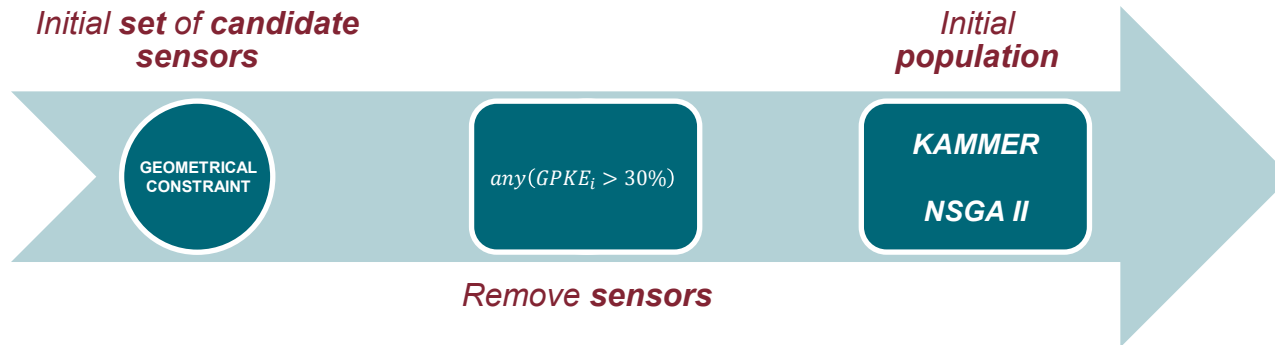
Reduce the initial population of candidate sensor locations \longrightarrow GPKE to discard points close to modal nodes

LOW SIGNAL-TO-NOISE RATIO

G.P.K.E. (*Grid Point Kinetic Energy*)

$$GPKE = \underbrace{\Phi_{pq} \sum_{s=1}^N M_{ps} \Phi_{sq}}_{\text{momentum associated with a given modal shape}} \longrightarrow \text{kinetic energy of a given mode shape associated with a specific degree of freedom}$$

momentum associated with a given modal shape





OPTIMAL SENSOR POSITIONING

KAMMER METHOD: *Mathematical Foundation* ①

Assumption (HP): Normal modes linearly independent

At least m independent measurements points required to identify m modes

$$\underline{u}_s = \underline{\Phi} \underline{q} \quad \begin{array}{l} \underline{u}_s : \text{measured structural displacements} \\ \underline{\Phi} : \text{mode shapes evaluated at sensor locations} \\ \underline{q} : \text{modal coordinates to estimate} \end{array}$$

$$\underbrace{\begin{bmatrix} \Phi_{11} & \cdots & \Phi_{1m} \\ \vdots & \ddots & \vdots \\ \Phi_{n1} & \cdots & \Phi_{nm} \end{bmatrix}}_{M \text{ modes}} \left. \vphantom{\begin{bmatrix} \Phi_{11} & \cdots & \Phi_{1m} \\ \vdots & \ddots & \vdots \\ \Phi_{n1} & \cdots & \Phi_{nm} \end{bmatrix}} \right\} N \text{ nodes}$$

Is it **BEST APPROACH** even with measurement **NOISE**?

It is possible to invert the relationship, but the matrix $\underline{\Phi}$ can be non square. **Least Square Estimator**

$$\underline{\hat{q}} = \left[\underline{\Phi}^T \underline{\Phi} \right]^{-1} \underline{\Phi}^T \underline{u}_s$$

PSEUDO-INVERSE

Why the pseudo-inverse?

Sensor placement gives $\underline{\Phi} \in \mathbb{R}^{N \times M}$, which is generally **rectangular**



OPTIMAL SENSOR POSITIONING

KAMMER METHOD: *Mathematical Foundation* ③

$$\underline{\underline{P}} = F \cdot I \cdot^{-1}$$

To optimize sensor placement, a **scalar measure** of the **Fisher Information Matrix** is required

A common choice is the **determinant**, leading to the following procedure:

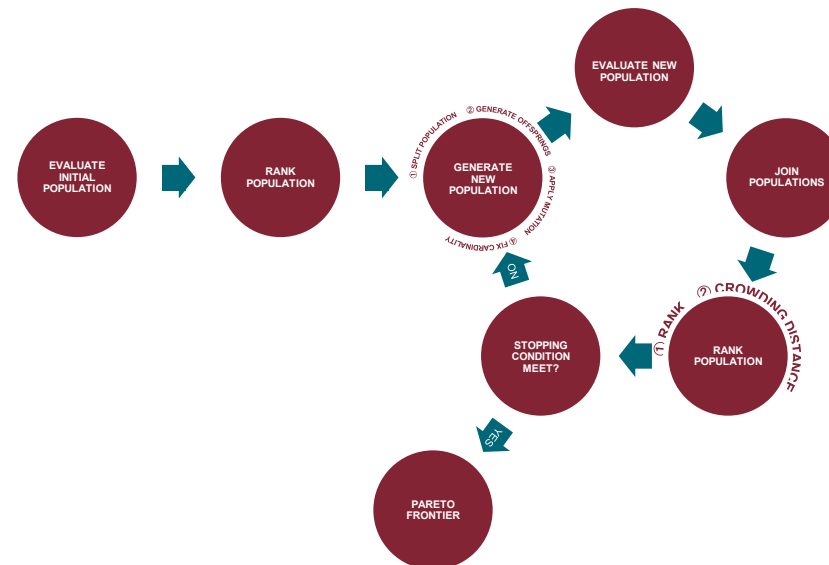
1. Compute the **eigenvectors** of $\underline{\underline{\Phi}}^T \underline{\underline{\Phi}}$ which coincide with $\underline{\underline{\Phi}}$ (*orthogonal modes for H_p*).
2. The **matrix** $\underline{\underline{\Phi}} \left[\underline{\underline{\Phi}}^T \underline{\underline{\Phi}} \right]^{-1} \underline{\underline{\Phi}}^T$ **quantifies** the **contribution** of each sensor location to the matrix **rank**
($\underline{\underline{\Phi}} [F.I.]^{-1} \underline{\underline{\Phi}}^T$ *Projection*)
3. Iteratively **remove** the **sensor locations contributing the least** to the **Fisher Information**, yielding the optimal sensor configuration for a given number of sensors N .



OPTIMAL SENSOR POSITIONING

GENETIC ALGORITHM

To better **explore** the **space of possible sensor configurations**
This approach exploits **mutation** and **crossover operators** to efficiently explore the design space



Sensor configurations are encoded using a binary mask, where 1 denotes an active sensor and 0 an inactive one



OPTIMAL SENSOR POSITIONING

GENETIC ALGORITHM: *Ranking and Selection*

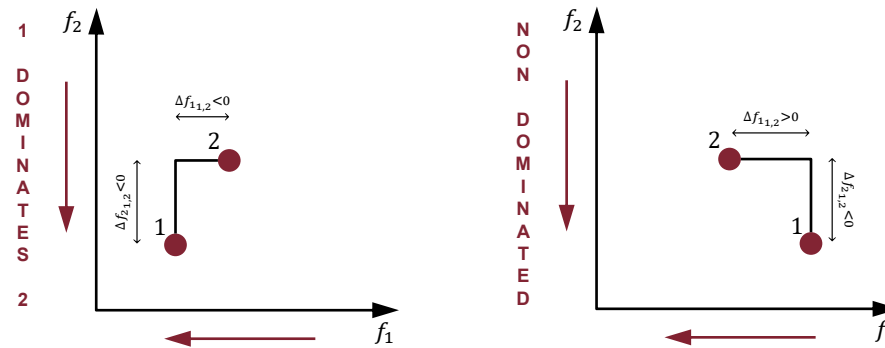
Ranking is assigned based on the concept of **dominance**

A solution is said to **dominate** another if it **performs** at least **as well** in **all objectives** and **strictly better** in **at least one objective**

A solution belongs to the **Pareto front (RANK 1)** if it is **not dominated by any other solution** in the design space

Solutions dominated by one or more **Pareto-optimal solutions** are assigned **higher ranks**. If a **solution** is **dominated by at least one solutions of rank n** , it is assigned **rank $n + 1$**

RANK POPULATION



5. OMA on REXUS36 Sounding Rocket

17/40



OPTIMAL SENSOR POSITIONING

GENETIC ALGORITHM: Crossover/Mutation

Once the **population** is **ranked**, it is randomly **split into two groups**

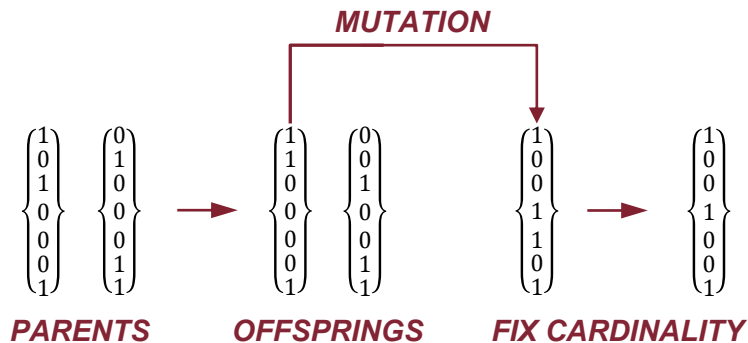
Each individual in **one group** is **paired with** an individual from **the other group**

The **paired individuals** are **combined to generate two offspring** with different genetic compositions (**crossover**)

Mutation is then **applied** to the offspring (*randomly change a/more gene/genes*)

To ensure that the **number of active sensors** remains **fixed**, **any excess sensors** are randomly **removed** (**fixed cardinality constraint**).

GENERATE NEW POPULATION



N° SENSORS = 3



OPTIMAL SENSOR POSITIONING

GENETIC ALGORITHM: *Joining Populations and Ranking*

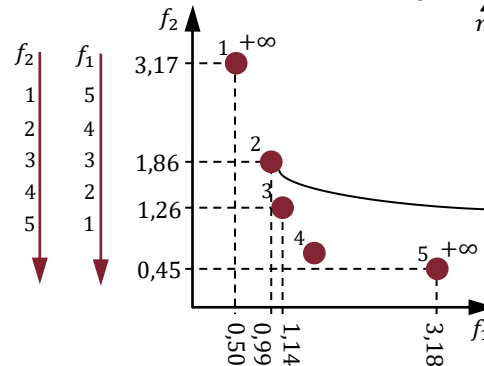
The **two populations** are **joined** and **ranked** based on **rank** and **crowding distance**

The **crowding distance** ensures **diversity among solutions** along the front and is **used to rank individuals** within the same rank.

Boundary solutions of each rank are assigned an **infinite crowding distance**.

The **remaining solutions** are **ranked** according to the **crowding distance**, computed after **sorting the solutions with respect to each objective**:

$$CD_p = \sum_{m=1}^M \frac{f_m(p_m^+) - f_m(p_m^-)}{f_m^{MAX} - f_m^{MIN}}$$



$$CD_2 = \frac{3,17 - 1,26}{3,17 - 0,45} + \frac{1,14 - 0,50}{3,18 - 0,50} = 0,94$$

GENERATE NEW POPULATION



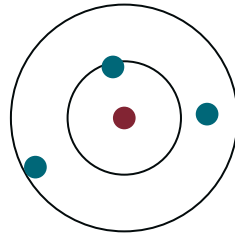
OPTIMAL SENSOR POSITIONING

GENETIC ALGORITHM: Objective Functions ①

① **MAC** (Modal Assurance Criterion) $\xrightarrow{\text{IDEAL}}$ \underline{I}

$$MAC = \frac{|\underline{\varphi}_i^T \underline{\varphi}_j|^2}{(\underline{\varphi}_i^T \underline{\varphi}_i)(\underline{\varphi}_j^T \underline{\varphi}_j)} \quad \Rightarrow \quad f_1 = \sqrt{\frac{1}{m(m-1)} \sum_{i=1}^M \sum_{j=1}^M MAC_{ij}^2 (i \neq j)}$$

② **ROBUSTNESS***



SENSOR LOCATION

MIS-PLACED SENSOR LOCATION $\rightarrow \Delta MAC$

50 analysis $\rightarrow f_2 = \max \Delta f_1$

***FEM uncertainties:** 5 analysis conducted for each of the 10 different models

OBJECTIVE FUNCTIONS



OPTIMAL SENSOR POSITIONING

GENETIC ALGORITHM: *Objective Functions* ②

Objective function: **MAC** for mass-varying systems

fuel consumption

11 mass models considered
($\Delta m = 29 \text{ kg}$ of propellant) \rightarrow radial burning

MAC evaluated for *each model*

The **MAC** is *integrated over time*
using the **trapezoidal rule**

$$\text{MINIMIZE} \sum_{i=1}^{11} \frac{(f_1^i + f_1^{i+1})}{2} \Delta t$$

Δt time span defined by fuel consumption

Fuel consumption defines the **duration**
of *each mass* configuration

OBJECTIVE FUNCTIONS

5. OMA on REXUS36 Sounding Rocket

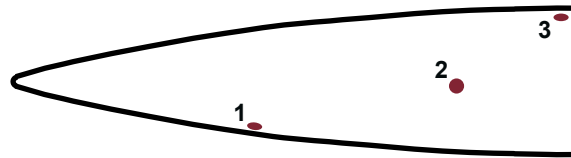


OPTIMAL SENSOR POSITIONING

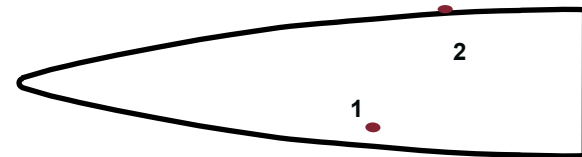
GENETIC ALGORITHM: *Constraint Functions*

CONSTRAINT FUNCTIONS

- ① **MAXIMUM 2** measurement point inside the nosecone (*limited number of pins*)

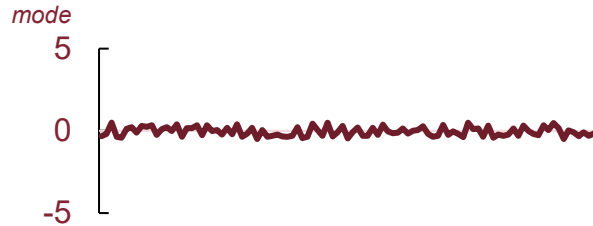


NOT FEASIBLE

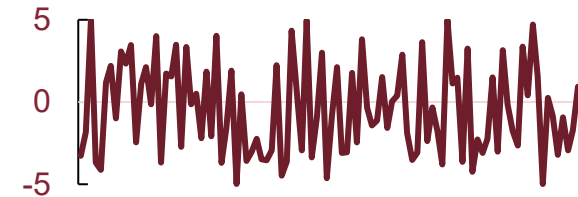


FEASIBLE

- ② **NO LOW ENERGY POINTS*** + at least 4 high-energy measurement points for each



AVOID



PREFER

***FEM uncertainties:** 5 analysis conducted for each of the 10 different models

5. OMA on REXUS36 Sounding Rocket






OPTIMAL SENSOR POSITIONING

REXUS ROCKET

The **REXUS** rocket is a **small sounding rocket**, approximately 6 meters long

FEM model → generated on the information provided in:

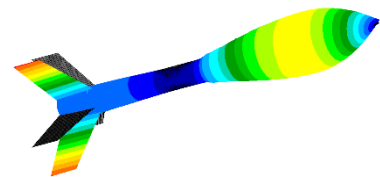
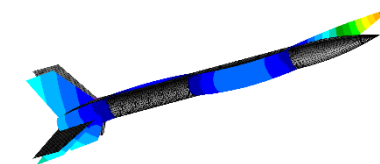
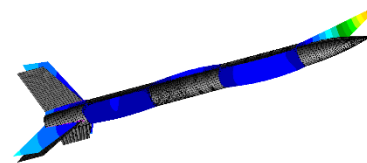
-  **REXUS/BEXUS User Manual**
-  **assumptions (previous launch campaigns)**
-  **typical reference values**

FE model → compute the structural mode shapes (**S.P.O.**)



E
S
S
E
N
T
I
A
L

A
C
C
U
R
A
T
E



R
S
E
Q
U
I
R
E
D
M
O
D
E
S

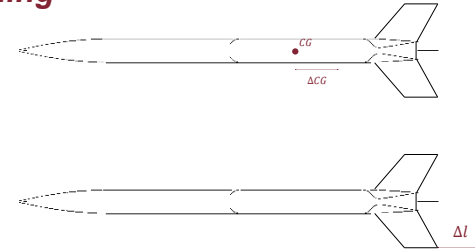


OPTIMAL SENSOR POSITIONING

REXUS ROCKET: *uncertainties modeling*

①

Motor mass distribution is uncertain
Internal balancing weight position is unknown



②

Mass and center-of-mass locations of the Recovery Module, Service Module, and Motor YoYo Adapter are unknown

Previous launch campaigns $\rightarrow \mu$ and σ

③

Material properties \rightarrow *YOUNG MODULUS* (500 MPa)
DENSITY (0.20 g/cm^3)
POISSON RATIO (0.03)

11 different randomly evaluated configurations for 11 mass cases (fuel consumption)

DEALING WITH UNCERTAINTIES



OPTIMAL SENSOR POSITIONING

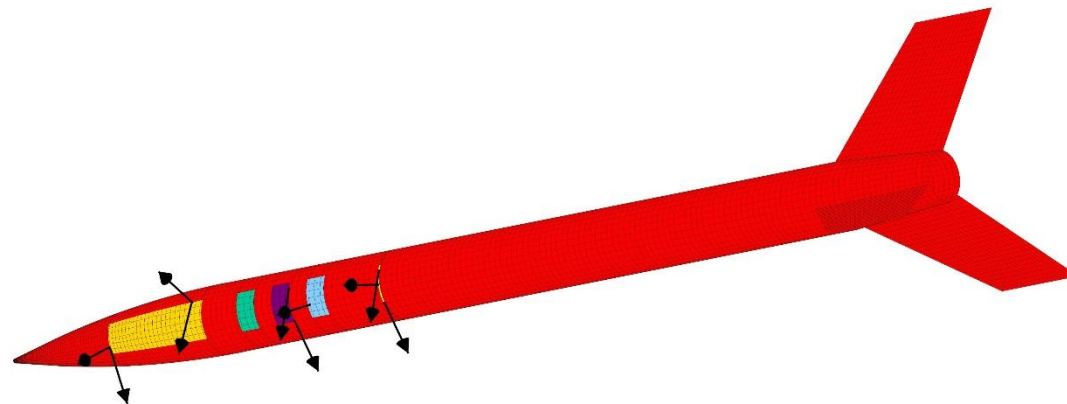
REXUS ROCKET: *sensor position optimization results (KAMMER)*

For each mass case, the **optimal sensor configuration** is identified



Optimal configuration minimizes the **time-integrated offMAC** (f_1)

$$\text{MINIMIZE} \sum_{i=1}^{11} \frac{(f_1^i + f_1^{i+1})}{2} \Delta t \quad \rightarrow \quad f_1 = \sqrt{\frac{1}{m(m-1)} \sum_{i=1}^M \sum_{j=1}^M MAC_{ij}^2 (i \neq j)}$$



OPTIMAL SENSOR PLACEMENT

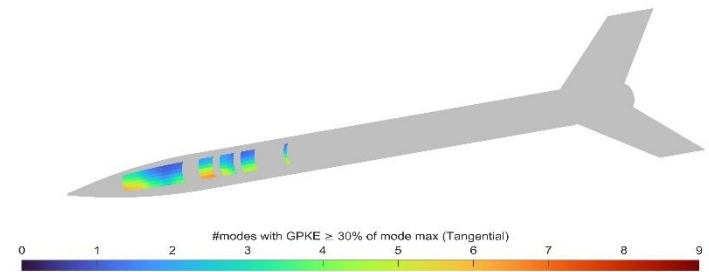
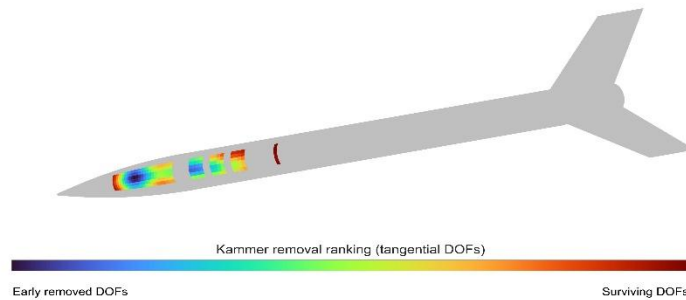
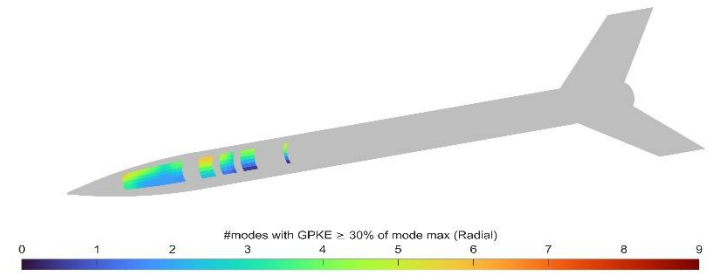
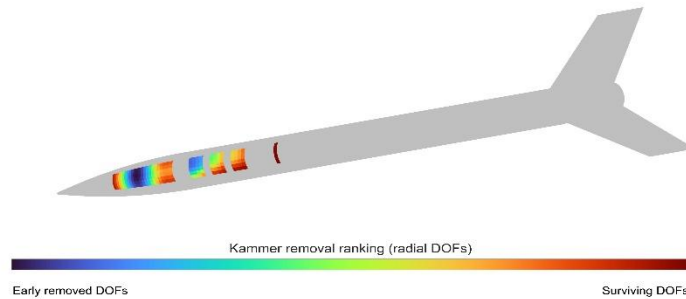
5. OMA on REXUS36 Sounding Rocket

25/40



OPTIMAL SENSOR POSITIONING

RESULTS: *Kammer*

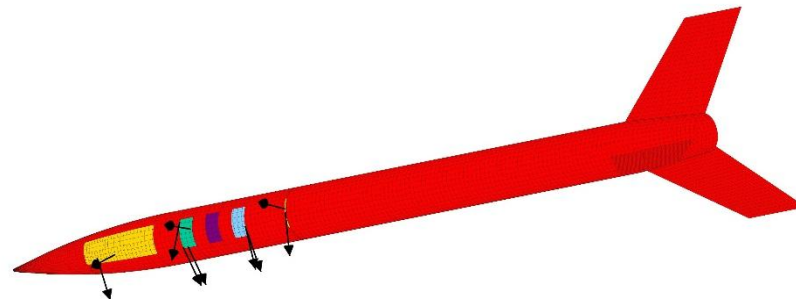
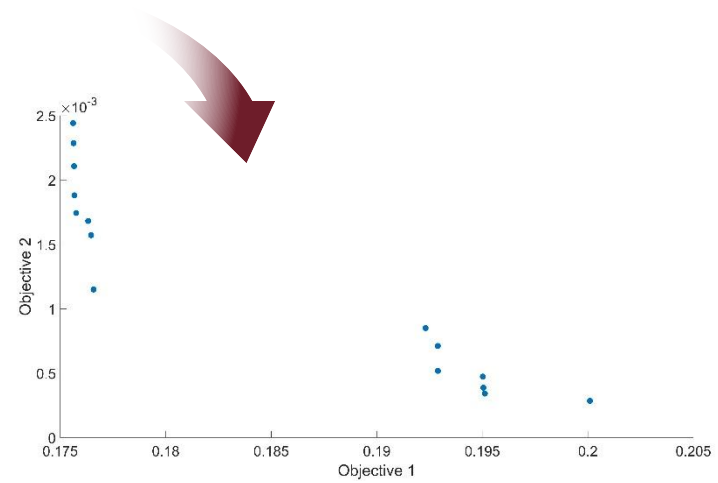
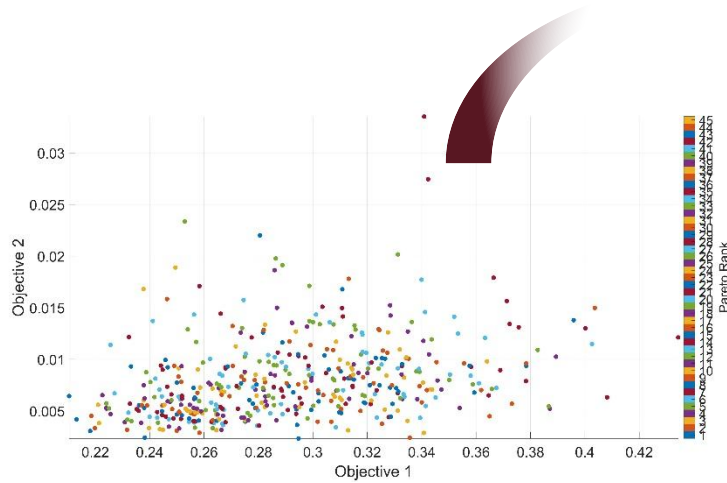


5. OMA on REXUS36 Sounding Rocket



OPTIMAL SENSOR POSITIONING

RESULTS: NSGA II



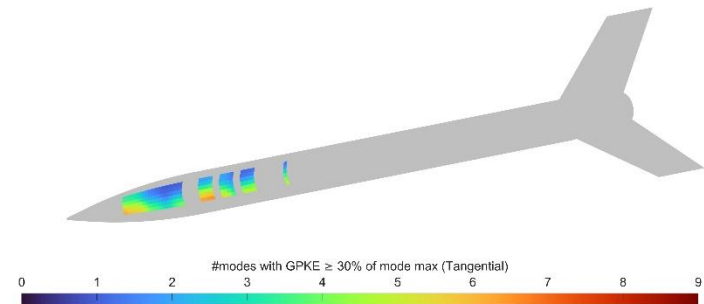
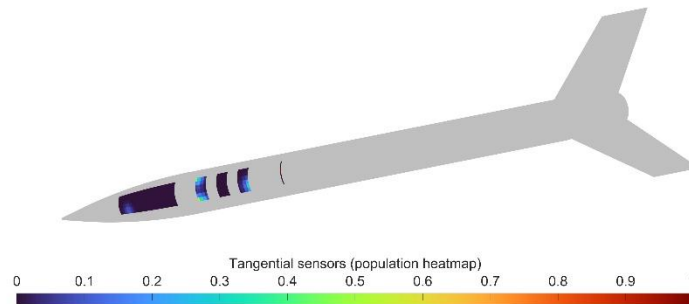
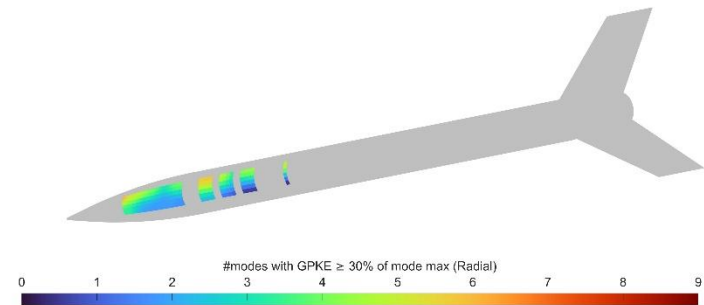
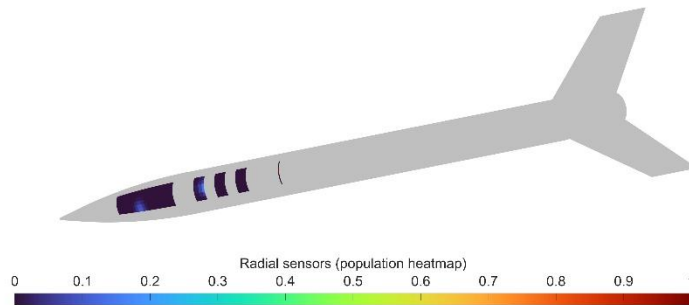
5. OMA on REXUS36 Sounding Rocket

27/40



OPTIMAL SENSOR POSITIONING

RESULTS: NSGA II



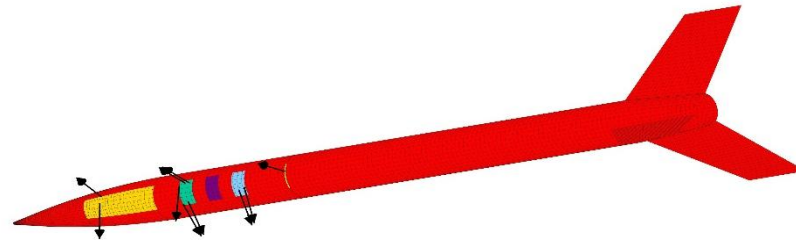
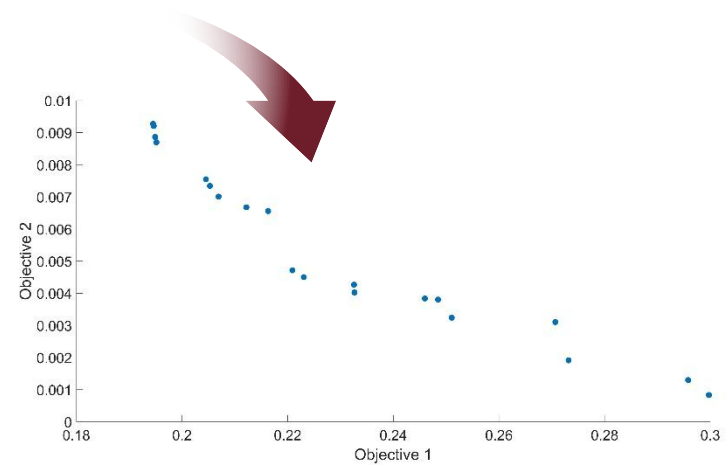
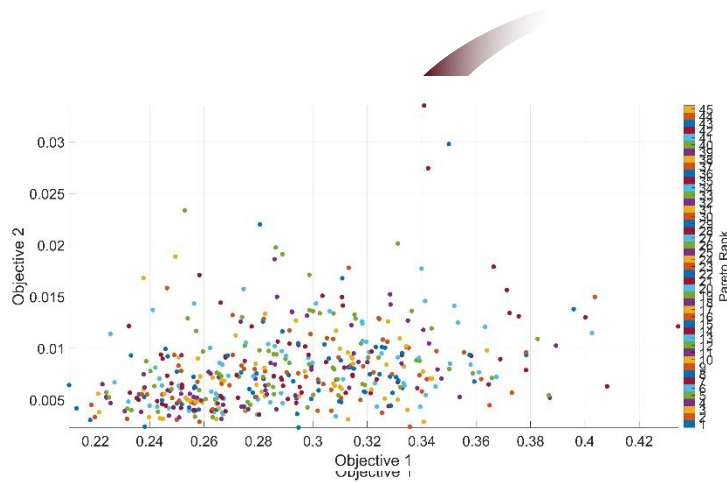
IOMAC2027 OMA Lectures: STRUCTURAL DYNAMICS EXPERIMENTS ON ESA SPACE LAUNCHERS

5. OMA on REXUS36 Sounding Rocket



OPTIMAL SENSOR POSITIONING

RESULTS: *NSGA II with uncertainties*



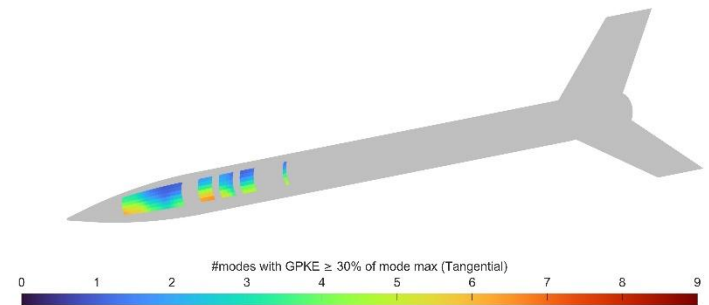
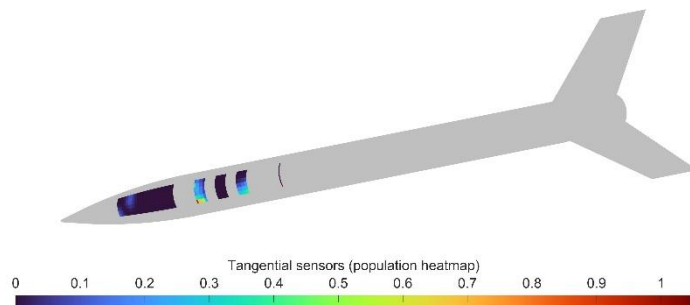
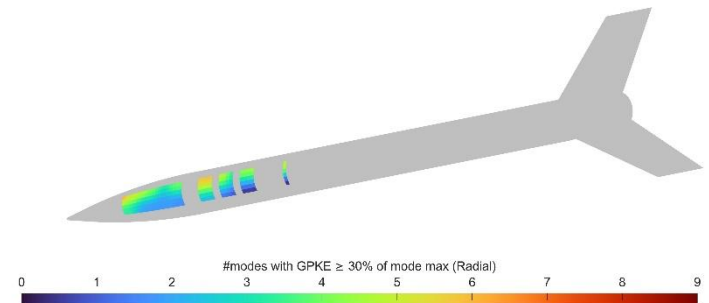
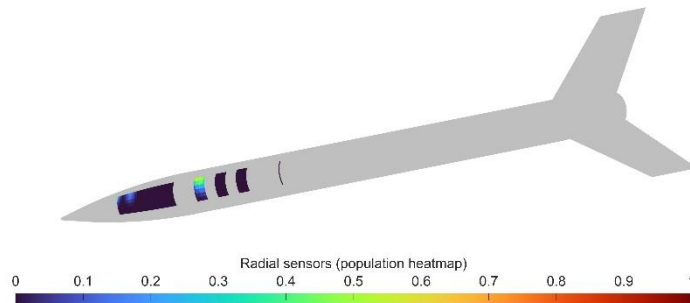
5. OMA on REXUS36 Sounding Rocket

29/40



OPTIMAL SENSOR POSITIONING

RESULTS: NSGA II with uncertainties





OPTIMAL SENSOR POSITIONING

RESULT:comparison

$$\textcircled{1} \quad \text{M.A.C.} \quad MAC = \frac{|\varphi_i^T \varphi_j|^2}{(\varphi_i^T \varphi_i)(\varphi_j^T \varphi_j)} \Rightarrow f = \sqrt{\frac{1}{m(m-1)} \sum_{i=1}^M \sum_{j=1}^M MAC_{ij}^2 (i \neq j)} \Rightarrow \sum_{i=1}^{11} \frac{(f_i^i + f_i^{i+1})}{2} \Delta t$$

$$\textcircled{2} \quad \text{G.P.K.E.} \Rightarrow g = \min_j \left(\text{mean}_i \left(\frac{GPKE_{i,j}}{\max_i(GPKE_{i,j})} \right) \right)$$

$\textcircled{3} \quad N_{\text{sensors}}(\text{NOSECONE})-2 \ (\leq 2 \text{ allowed})$

$\textcircled{4} \quad N_{\text{sensors}}(\text{G.P.K.E.} < 30\%) \ (\text{Sensors below energy threshold})$

$\textcircled{5} \quad \max(\Delta\textcircled{1})$

$\textcircled{6} \quad N_{\text{MODES}}$ with fewer than 4 sensors exceeding the G.P.K.E. threshold (30%), accounting for uncertainties

METRICS

	①	②	③	④	⑤	⑥	ΔT
KAMMER	0.2294	0.1907	1	7	0.0059	1	1.7 s
NSGA II	0.1756	0.2256	0	0	0.0098	1	1717 s
NSGA II <i>with uncertainties</i>	0.1945	0.2164	0	0	0.0093	0	3054 s

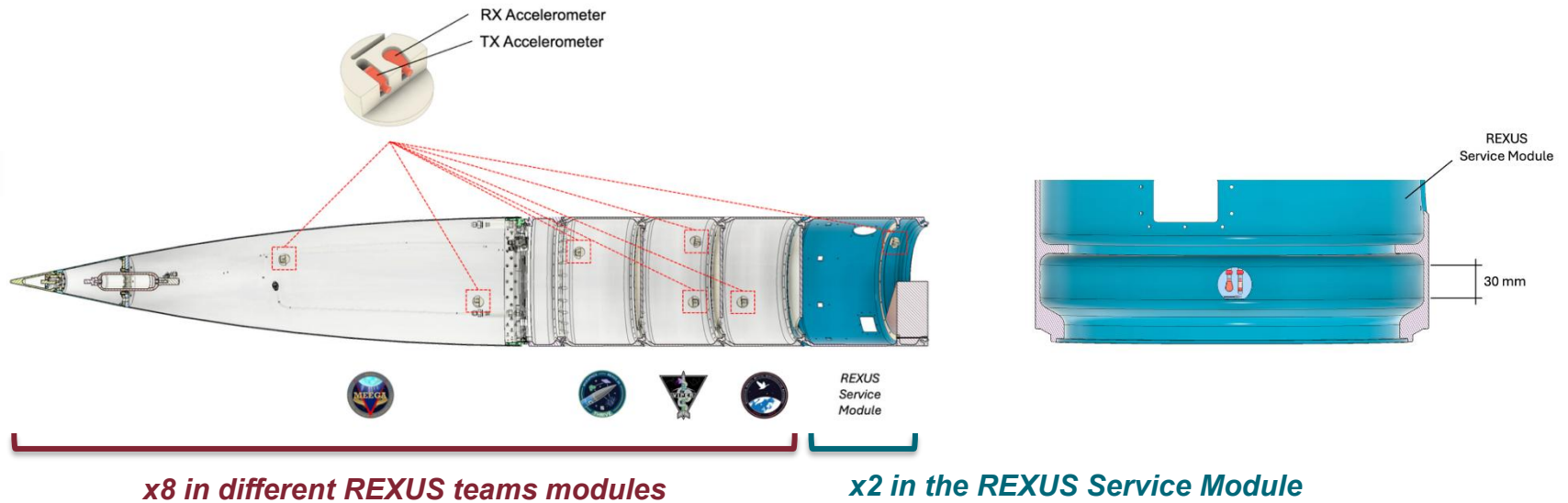
5. OMA on REXUS36 Sounding Rocket

31/40



OPTIMAL SENSOR POSITIONING

RESULT: optimal configuration



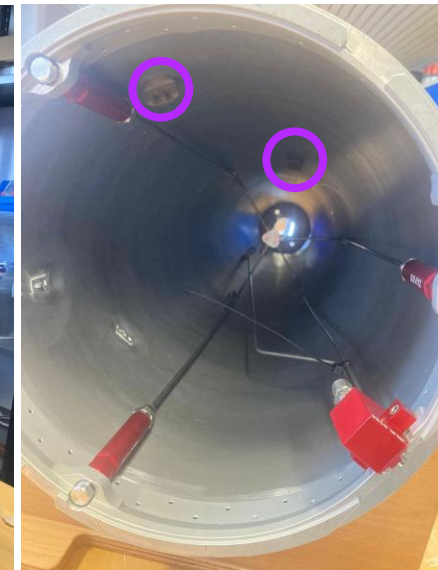
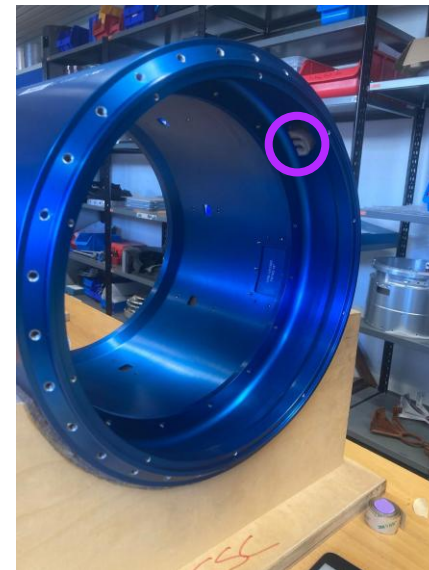
5. OMA on REXUS36 Sounding Rocket

32/40



OPTIMAL SENSOR POSITIONING

RESULT: sensor installation



IOMAC2027 OMA Lectures: STRUCTURAL DYNAMICS EXPERIMENTS ON ESA SPACE LAUNCHERS

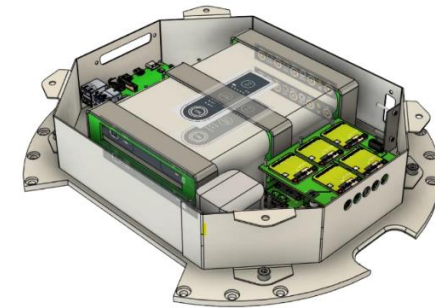
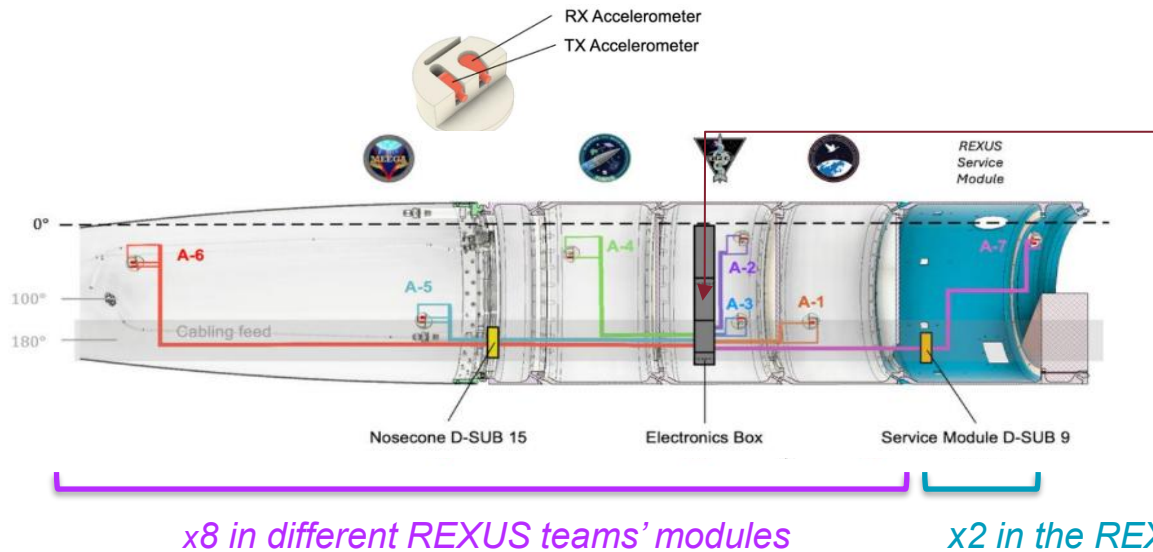
Dept. of Mechanical and Aerospace Engineering – University of Rome «La Sapienza», Roma, Italy
April 09, 2026

5. OMA on REXUS36 Sounding Rocket

33/40



MEASURING CHAIN DESIGN



x2 SCADAS in the electronic box in VIPER module

The accelerometer will be mounted all over the payload area of the Rexus-36 launcher. The cable interfaces was carefully designed to guarantee: quick disconnection of the different modules, mounting of the accelerometers without cables already connected, nosecone ejection, minimal noise interference and optimal signal quality



MEASURING CHAIN DESIGN

TESTING

Tests aims to verify the SCADAS XS functionality under vibration levels exceeding its design specifications.

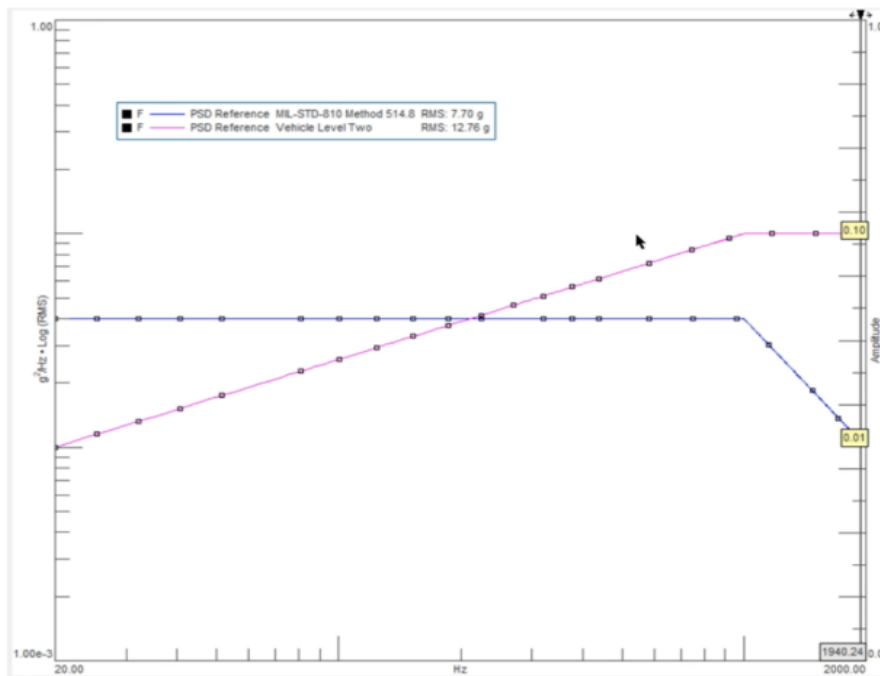


Figure 3 – Random Vibration PSD comparison between SCADAS XS Qualification Level and RX Level 2

The system maintains proper functionality under vibration levels exceeding its qualification profile, while the supports effectively secure the SCADAS without structural degradation.

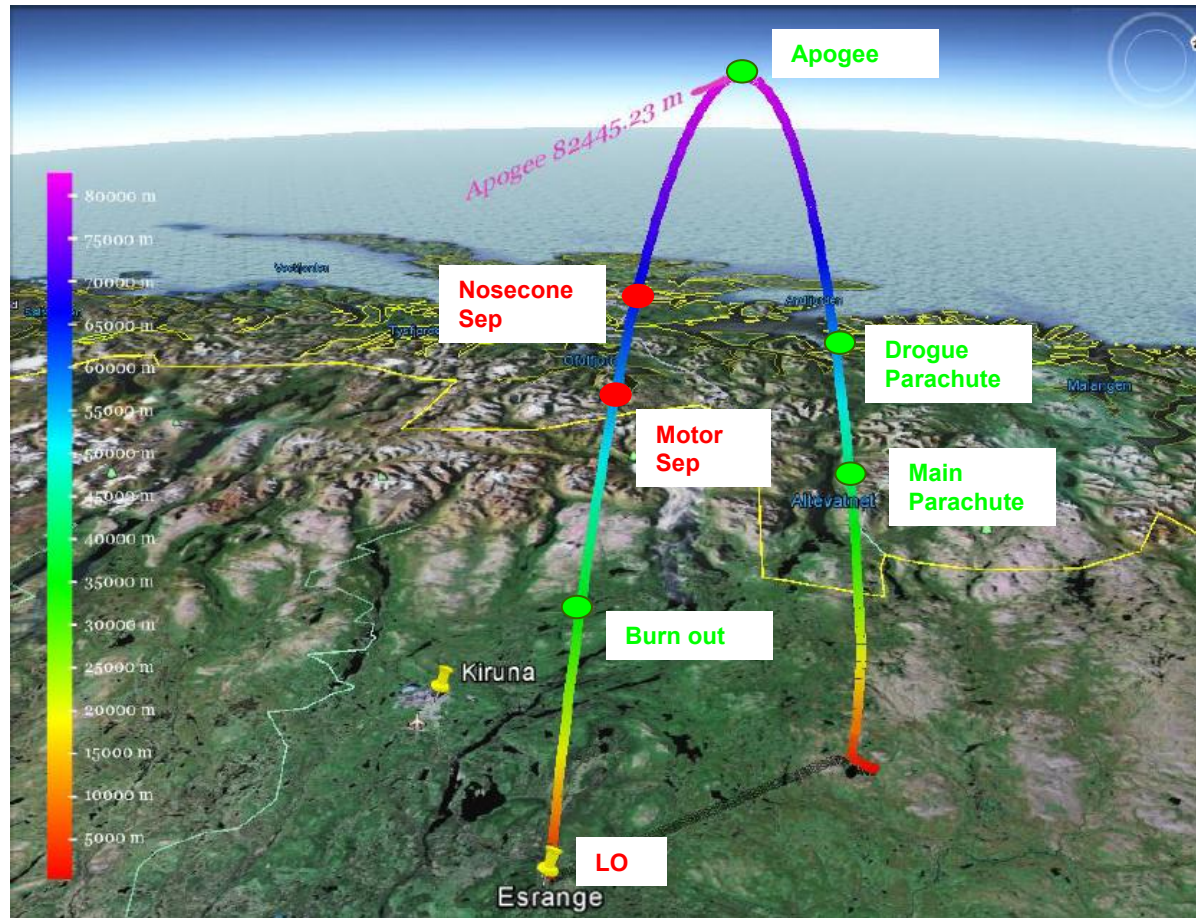
5. OMA on REXUS36 Sounding Rocket

35/40



PRELIMINARY RESULTS

FLIGHT ENVELOPE



IOMAC2027 OMA Lectures: STRUCTURAL DYNAMICS EXPERIMENTS ON ESA SPACE LAUNCHERS

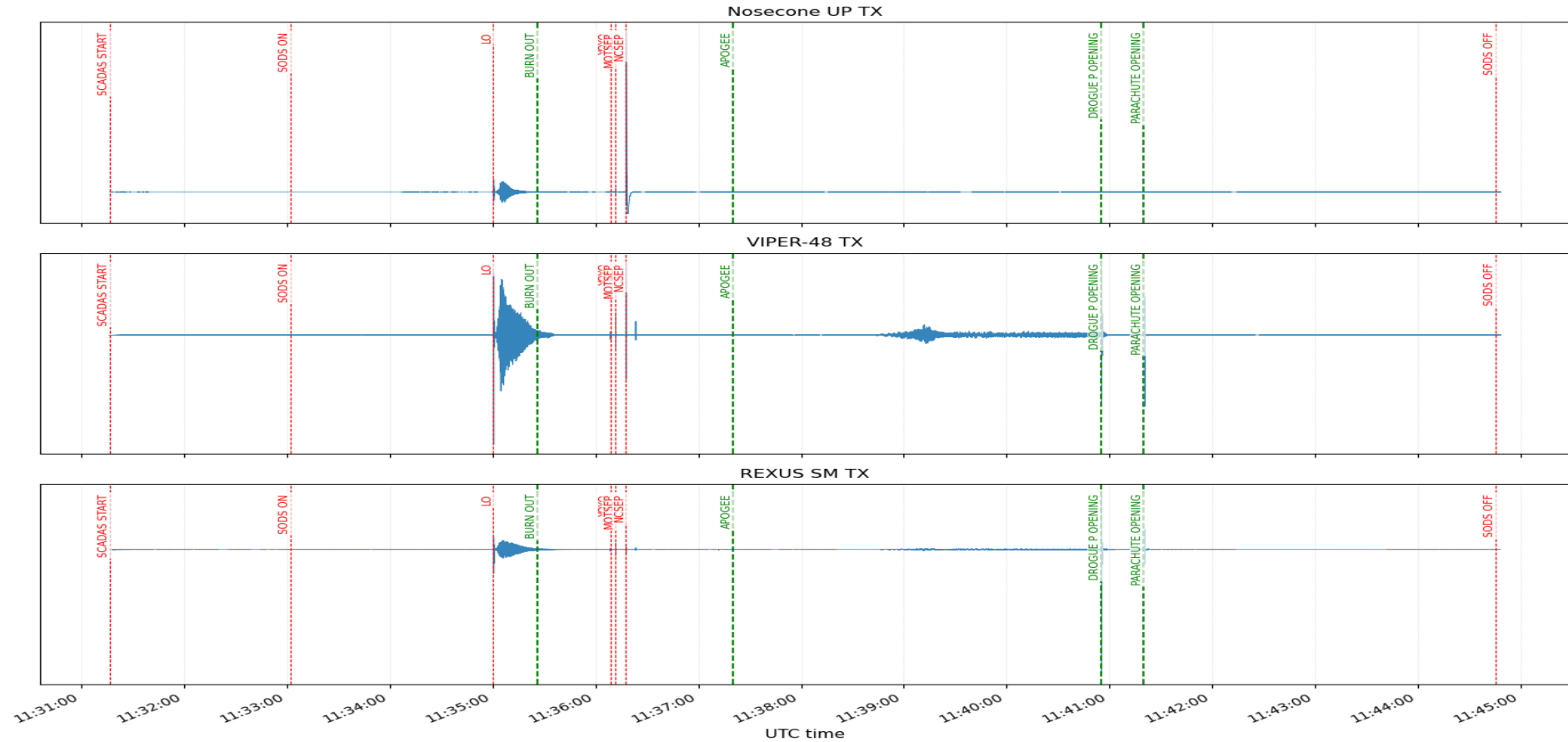
5. OMA on REXUS36 Sounding Rocket

36/40



PRELIMINARY RESULTS

RECORDED ACQUISITIONS WITH FLIGHT'S EVENTS



IOMAC2027 OMA Lectures: STRUCTURAL DYNAMICS EXPERIMENTS ON ESA SPACE LAUNCHERS

5. OMA on REXUS36 Sounding Rocket

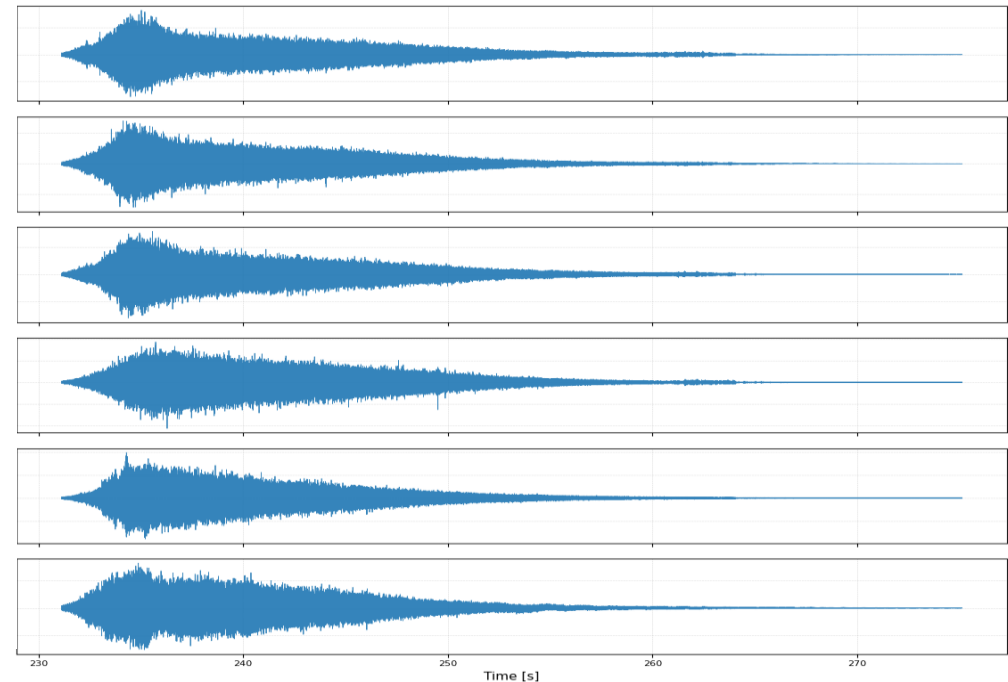
37/40



PRELIMINARY RESULTS

OMA ANALYSIS PARAMETERS DURING BURN OUT PHASE

- OMA method: SSI
- Number of samples: 32768
- Number of blocks for overlap: 16
- Overlap percentage: 50%
- Vandermonde order: 80
- Stabilization diagram order: 100



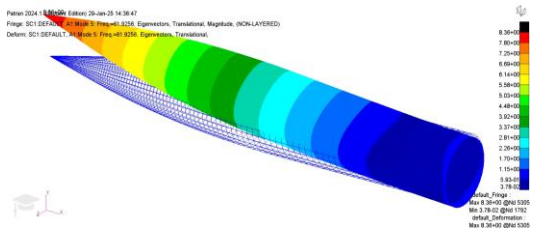
5. OMA on REXUS36 Sounding Rocket



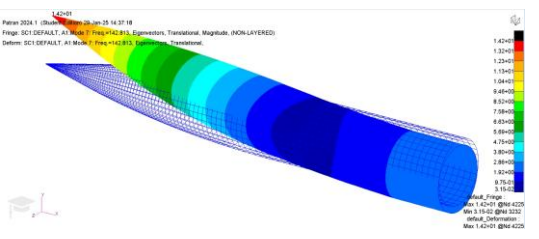
PRELIMINARY RESULTS

COMPARISON OF THE FIRST 3 MODE SHAPES: FEM vs OMA ANALYSIS

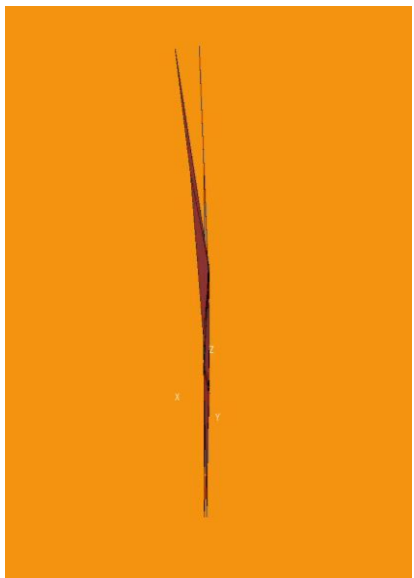
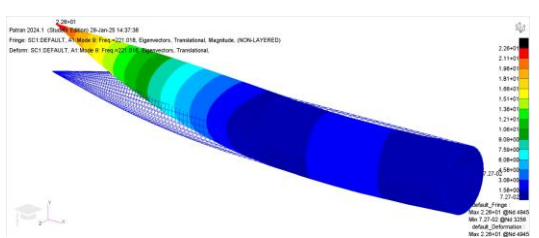
$f = 61.58 \text{ Hz}$



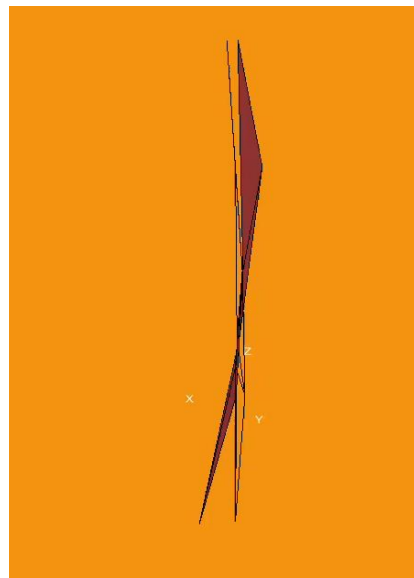
$f = 142.91 \text{ Hz}$



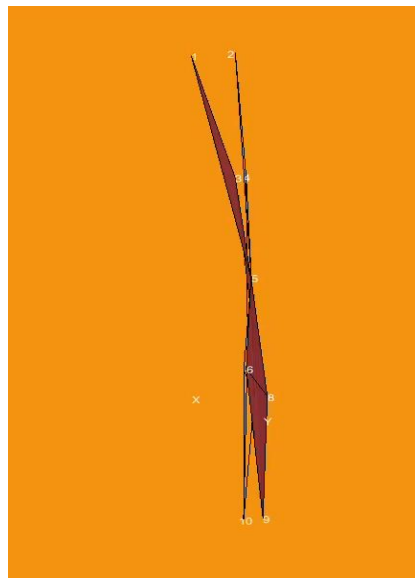
$f = 221.43 \text{ Hz}$



$f = 44,57 \text{ Hz}$



$f = 114,35 \text{ Hz}$



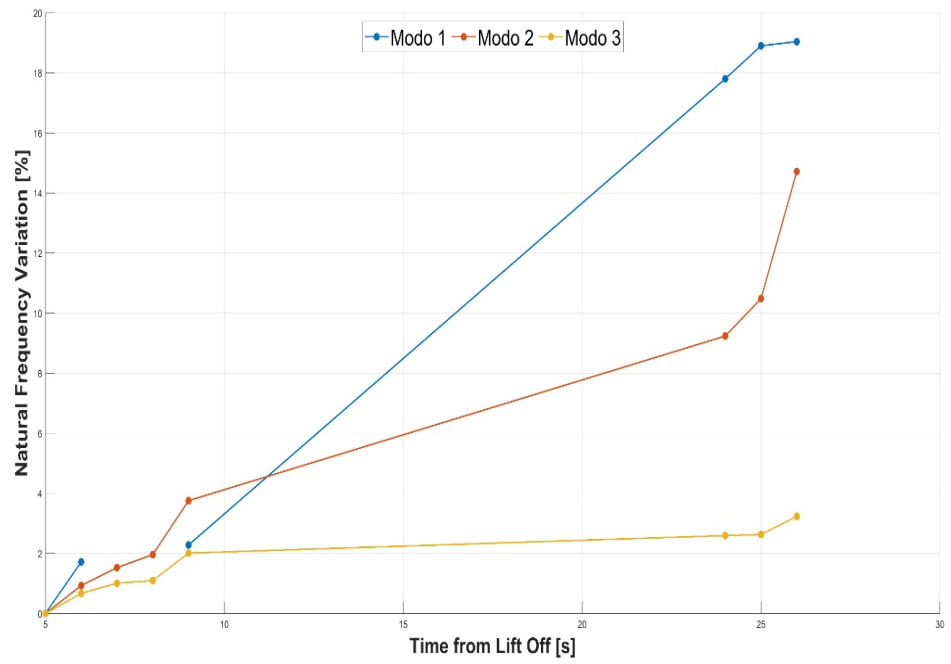
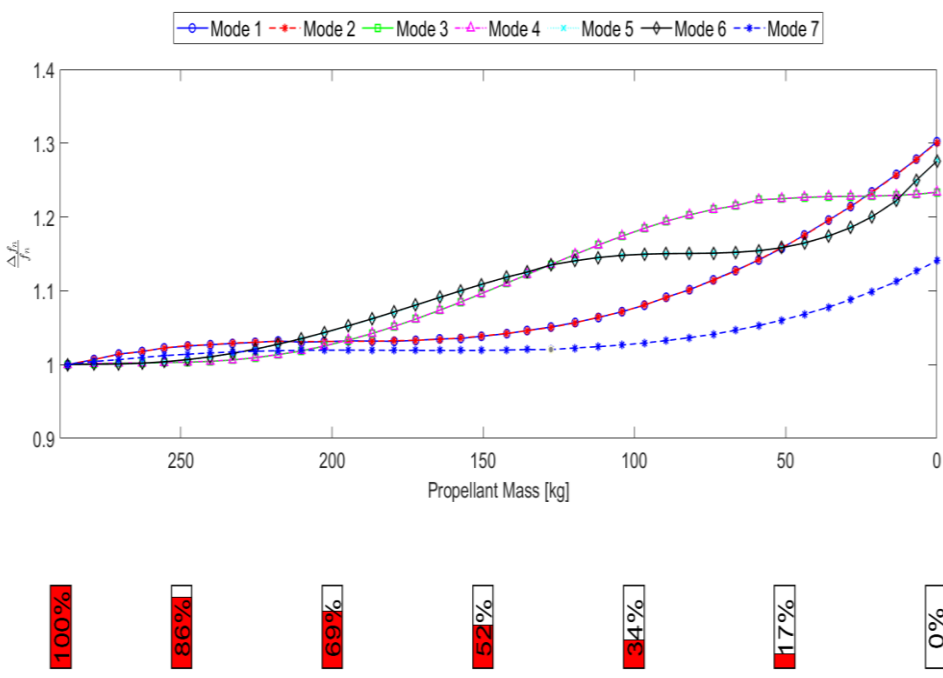
$f = 194,79 \text{ Hz}$

5. OMA on REXUS36 Sounding Rocket



PRELIMINARY RESULTS

COMPARISON of NATURAL FREQUENCY VARIATION DURING BURN OUT: FEM vs OMA ANALYSIS



5. OMA on REXUS36 Sounding Rocket

40/40



FUTURE DEVELOPMENTS

THERE IS STILL MUCH WORK TO BE DONE

- Implementation of pre-processing techniques to enhance data quality for OMA analysis
- Application of multiple OMA methods for sensitivity assessment
- Further investigations of dynamic behaviour during :
 1. propelled flight
 2. burn out phase
 3. ballistic flight
- Re-entry phase analysis correlated with IMU-derived velocity profiles
- Possible interactions with controlled systems and on board hardwares or payload
- OMA technologies exploitation for larger commercial launch vehicles

Agenda

1. Motivations
2. Theoretical Background on OMA approaches
3. OMA on ARIANE Launch Vehicle
4. OMA on VEGA P80 Motor
5. OMA on REXUS36 Sounding Rocket
6. Concluding Remarks

- The considered OMA methods (FDD, HTM – but also SSIs) **provide a time-tracking** of the modal properties of the considered launch system
- The system natural frequencies are time-tracked with practically **the same behavior**
- The **damping ratios** behavior seems to be **dependent** on the chosen **method** and on the **analysis parameters**. However, by considering the system poles as representative of the system dynamics the **methods give consistent results**
- The considered methods are **able to time-track the mode shapes** even if for **higher order modes are required more samples and measure points**
- It is relevant to point out that even if **the identification can fail** for some intervals within the same method, the **synergic use of the methods provides the complete tracking** of the modal properties of the studied system

- The developed **sensor placement method** reveals itself as a very **useful tool** for the test planning and for the mode shape identification phases
- **Uncertainties from OMA** analysis are **comparable** with those from the **standard EMA**, in which both the input and output signals are measurable
- The **OMA also allows** to evaluate the so-called **operational modes** due to harmonic excitations caused by the inner dynamics of the system, that the **standard experimental tests do not induce**

Acknowledgements

The authors gratefully acknowledge the contributions of the following individuals to this presentation:

Prof. Alessandro Agneni
Prof. Luigi Balis Crema
Prof. Franco Mastroddi
Prof. Paolo Gaudenzi
Dr. Chiara Grappasonni
Prof. Cristina Riso
Dr. Marco Eugeni
Eng. Valerio Spadoni
Eng. Tommaso Pantalani

And all the VIPER student Team



IOMAC2027 OMA Lectures: STRUCTURAL DYNAMICS EXPERIMENTS ON ESA SPACE LAUNCHERS

Reading list

- S.P. Timoshenko and J.N. Goodier, "Theory of Elasticity," International Student Edition.
- S.P. Timoshenko and S. Woinowsky-Krieger, "Theory of Plates and Shells," McGraw-Hill International Editions.
- P.C. Chou and N.J. Pagano, "Elasticity - Tensor, Dyadic and Engineering Approaches," Dover Publications, Inc.
- H. Megson, "Aircraft Structures for engineering Students," Elsevier Aerospace Engineering.
- C.T. Sun, "Mechanics of Aircraft Structures," Wiley
- J.S. Przemieniecki, "Theory of Matrix Structural Analysis," Dover Publications, Inc.
- M.C.Y Niu, "Airframe Structural Design; Practical Design Information," Conmilit.
- O.C. Zienkiewicz, R.L. Taylor, J.Z. Zhu, "the Finite Element Method," Butterworth-Heinemann.
- K.J. Bathe, "Numerical Methods in Finite Element Analysis," Prentice-Hall.
- L. Meirovitch, "Computational Methods in Structural Dynamics," Sijthoff & Noordhoff Ed.
- Beckwith, T.G., Marangoni, R.D., Mechanical Measurements, Addison-Wesley Publishing Company 1990.
- Bendat, J.S., Piersol, A.G., Random Data, John Wiley and Sons, Inc., 2nd edition, 1986.
- Shin, K, Hammond, J.K., Fundamentals of Signal Processing for Sound and Vibration Engineers, Wiley, 2008.
- Pintelon, R., Schoukens, J., System Identification: A Frequency domain Approach, Institute of Electrical and Electronics Engineers, Inc., 2001.
- E.A. Robinson, M.T. Silva, Digital Signal Processing and Time Series Analysis, San Francisco, CA, USA, 1978.
- L. Meirovitch, Elements of Vibration Analysis, McGraw-Hill, II Edition (1986).
- C. Hatch, G.W. Skingle, C.H. Greaves, N.A.J. Lieven, J.E. Coote, M.I. Friswell, J.E. Mottershead, H. Shaverdi, C. Mares, A. McLaughlin, M. Link, N. PietLahanier, M.H. Van Houten, D. G"oge, H. Rottmayr, Methods for Refinement of Structural Finite Element Models: summary of the GARTEUR AG14 collaborative programme, in: Proceedings of the 32nd European Rotorcraft Forum, 2006.
- Ewins, D.J., Modal Testing: Theory, Practice and Application, Research study press LTD, John 2000.
- He, J., Fu ZF., Modal Analysis, Butterworth-Heinemann, 2001.
- Heylen W., Lammens S., Sas P., Modal Analysis Theory and Testing, KU Leuven, 2007.
- Inmann, D.J., Vibration with Control, Wiley, 2006.

- L. Hermans, H. Van der Auweraer, Modal testing and analysis of structures under operational conditions: industrial applications, *Mechanical Systems and Signal Processing*, 13 (2) (1999) 193-216.
- F. Poncelet, G. Kerschen, J.-C. Golinval, D. Verhelst, Output-only modal analysis using blind source separation techniques, *Mech. Syst. Signal Process.* 21 (6) (2007) 2335–2358, <http://dx.doi.org/10.1016/j.ymssp.2006.12.005>.
- R. Brincker, C.E. Ventura, P. Andersen, Damping estimation by frequency domain decomposition, in: XIX IMAC, Kissimee, FL, USA, 2001.
- R. Brincker, L. Zhang, P. Andersen, Modal Identification from Ambient Responses Using Frequency Domain Decomposition, XVIII IMAC, S. Antonio, TX, (USA), , Society for Experimental Mechanics, Inc., Bethel, CT, USA, pp. 625-630(2000).
- P. Van Overschee, B. De Moor, 1996. Subspace Identification for Linear Systems, Kluwer Academic Publisher.
- A. Agneni, L. Balis Crema, G. Coppotelli, (2010), Output-Only Analysis of Structures with Closely Spaced Modes, *Mechanical System and Signal Processing. Special Issue: Operational Modal Analysis*, Vol 24, N. 5, July, pp. 1240-1249.
- N. Ameri, C. Grappasonni, G. Coppotelli, D.J. Ewins, Ground vibration tests of a helicopter structure using OMA techniques, *Mechanical Systems and Signal Processing*, Volume 35, Issues 12, 2013, Pages 35-51, ISSN 0888-3270, <https://doi.org/10.1016/j.ymssp.2012.09.013>. (<https://www.sciencedirect.com/science/article/pii/S0888327012003718>).
- J. Covioli, G. Coppotelli, (2021). On the use of Gaussian Mixture Models for Automated Modal Parameters Estimation. AIAA Scitech 2021 Forum, January 2021, 10.2514/6.2021-1035.
- F. Mastroddi, G. Coppotelli, G.M. Polli, C. Di Trapani, Vibro-Acoustic Response Analysis to Pressure Oscillations in a Solid Rocket Motor - Comparison with the Experimental Fire-Test Data, *Aerotecnica Missili e Spazio*, ISSN 0365-7442, (2007)
- SIEMENS LMS Test.LAB, Theoretical and User Manuals
- ECSS-E-HB-10-02A – Verification guidelines (17 December 2010)
- ECSS-E-HB-10-03A – Testing guidelines (31 May 2022)
- ECSS-E-HB-32-25A: Mechanical shock design and verification handbook (14 July 2015)
- ECSS-E-HB-32-26A: Spacecraft mechanical loads analysis handbook (19 February 2013)

THE END!



IOMAC2027 OMA Lectures: STRUCTURAL DYNAMICS EXPERIMENTS ON ESA SPACE LAUNCHERS

Dept. of Mechanical and Aerospace Engineering – University of Rome «La Sapienza», Roma, Italy
April 09, 2026

G. Coppotelli, D. Antonini, L. Onofri